The Solar Dynamo Saga: Chapter12

David Hathaway
NASA Marshall Space Flight Center

2011 December 12 – NSO

http://solarscience.msfc.nasa.gov/presentations.html

Outline

- Key Characteristics of the Sunspot Cycle
- The Solar Dynamo Saga:
  - The first 100 years
- Chapter 11:
  - Why Flux Transport Dynamos are Bankrupt
- Chapter 12:
  - Directions out of Bankruptcy

The Sunspot Cycle

http://solarphysics.livingreviews.org/Articles/lrsp-2010-1/

Sunspot Cycle Discovery

Astronomers had been observing sunspots for over 230 years before Heinrich Schwabe, an amateur astronomer in Dessau, Germany, discovered in 1844 that the number of sunspot groups and the number of days without sunspots increased and decreased in cycles of about 10-years.

Schwabe's data for 1826 to 1843

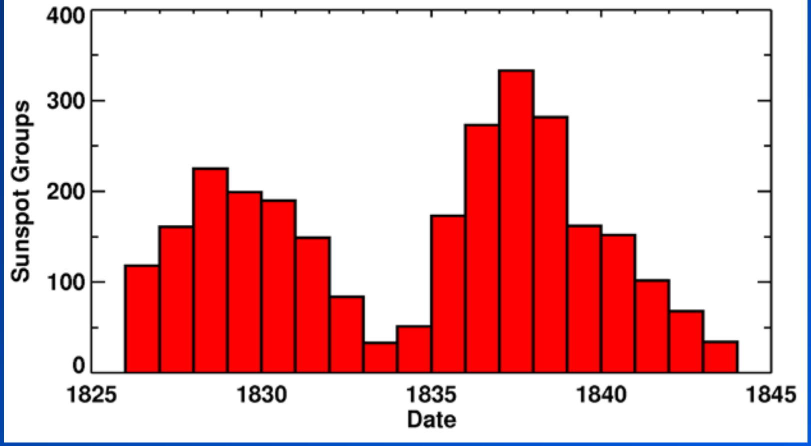

Number of Sunspot Groups per Year

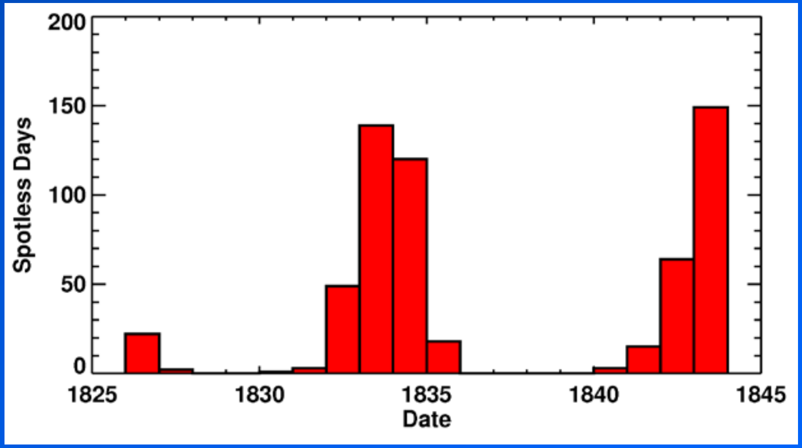

Number of Spotless Days

23 Cycles and Counting

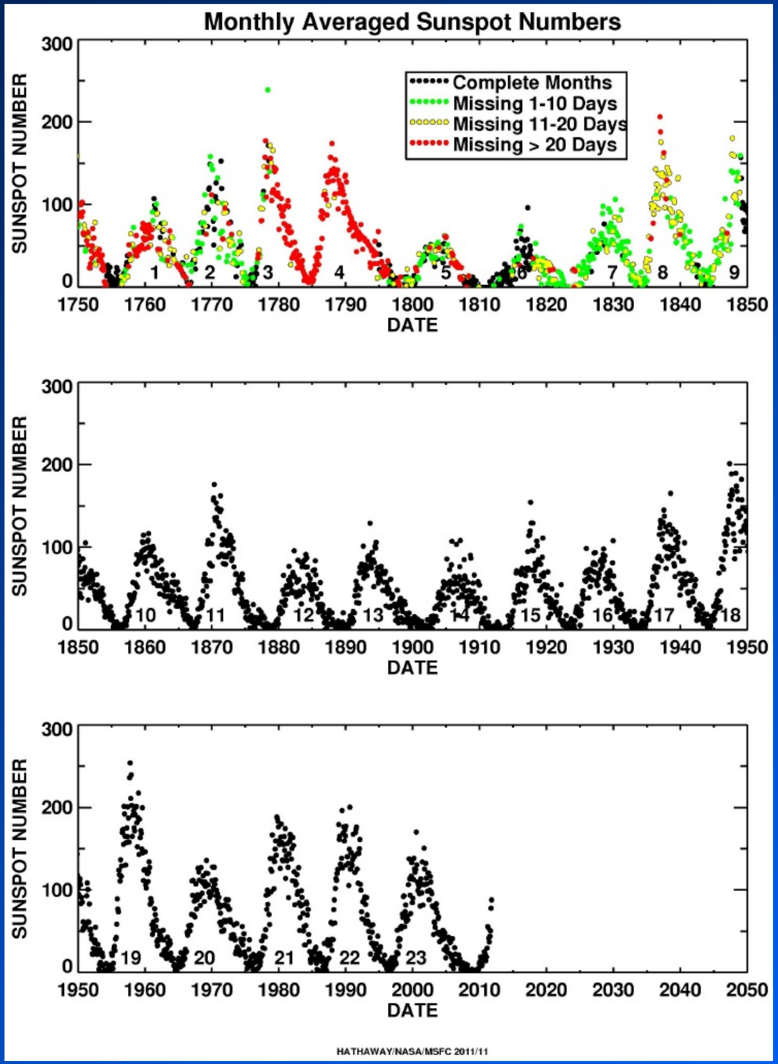

Shortly after Schawbe's discovery Rudolf Wolf proposed using a "Relative" Sunspot Number count:

$$R = k\,(10\,g + n)$$

Where *k* is a correction factor (~0.6) *g* is the number of sunspot groups and *n* is the number of spots

The average cycle lasts about 11 years with a range from 9 to 14.

The average amplitude is about 100 with a range from 50 to 200.

The Maunder Minimum

The “Maunder Minimum” – a period of 70 years with virtually no sunspots - was first identified by Gustav Spörer as reported by E. Walter Maunder to the Royal Astronomical Society in 1890. It was thought for decades that this was due to a lack of observations. Jack Eddy revived interest in the Maunder Minimum in 1976. Doug Hoyt and Ken Schatten searched through sunspot observation records from 1610 to 1750 and confirmed the existence of the Maunder Minimum in 1998.

In addition to grand minima like the Maunder Minimum, there appears to be a long-term periodicity of about 100 years in cycle amplitudes.

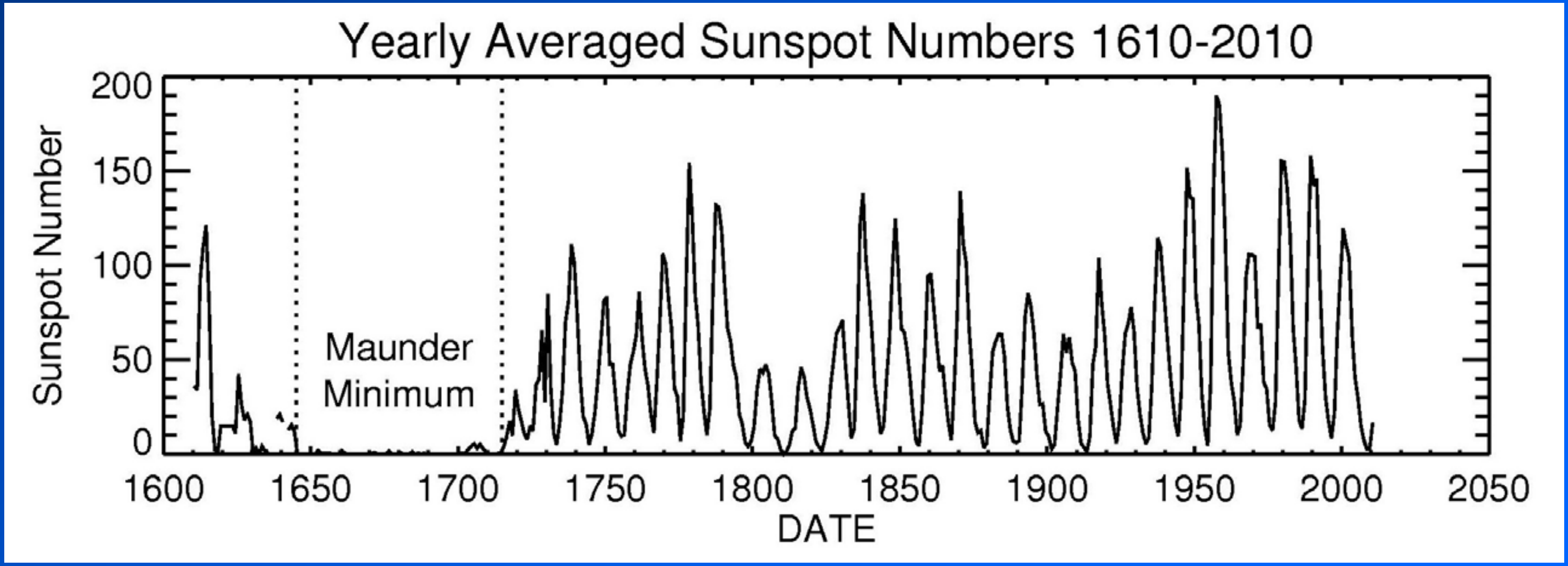

The Waldmeier Effect

Waldmeier (1935) noted that the sunspot cycles, as measured by the sunspot number, are asymmetric with a faster rise to maximum and a slower decline to minimum. This asymmetry is heightened in larger cycles. **Big cycles take less time to rise from minimum to maximum.**

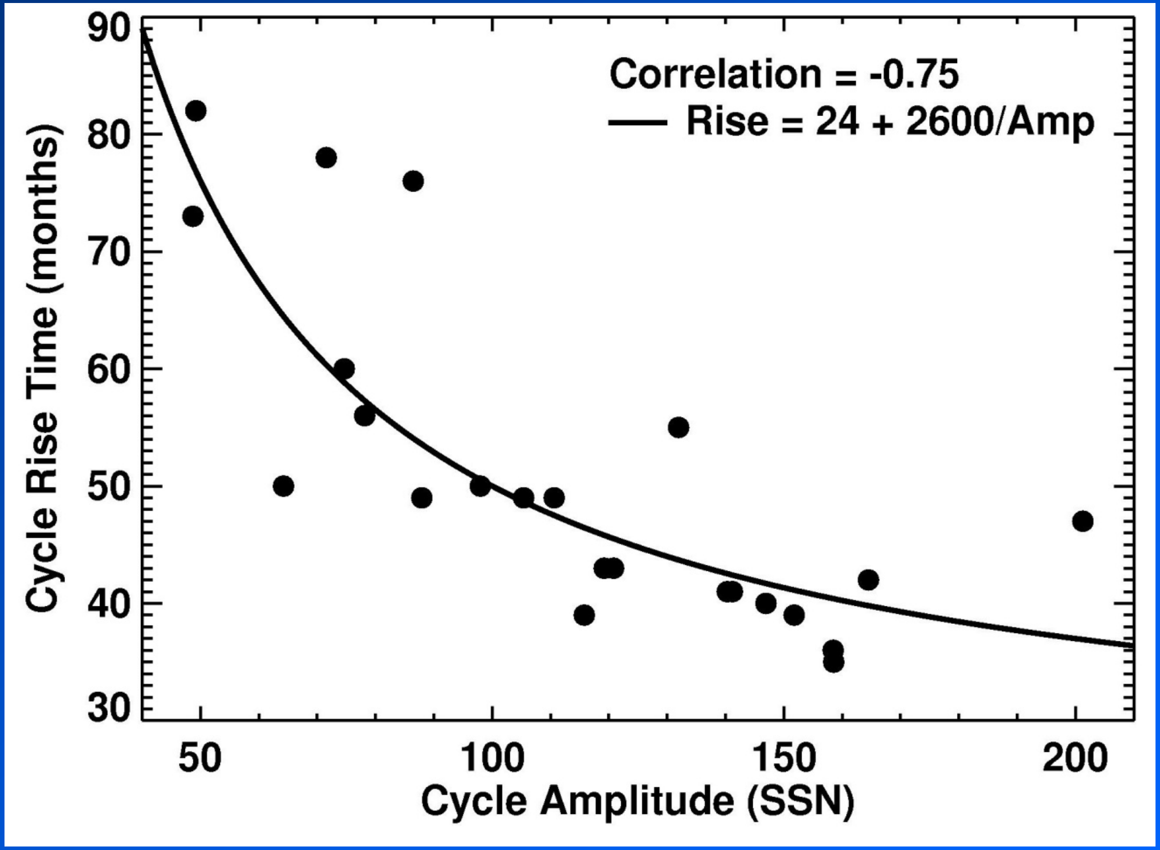

Sunspot Zones

Sunspots appear in two latitude zones, one in the north and one in the south. These zones drift toward the equator as each cycle progresses. Big cycles have wider zones that extend to higher latitudes. Cycles can overlap by 2-3 years.

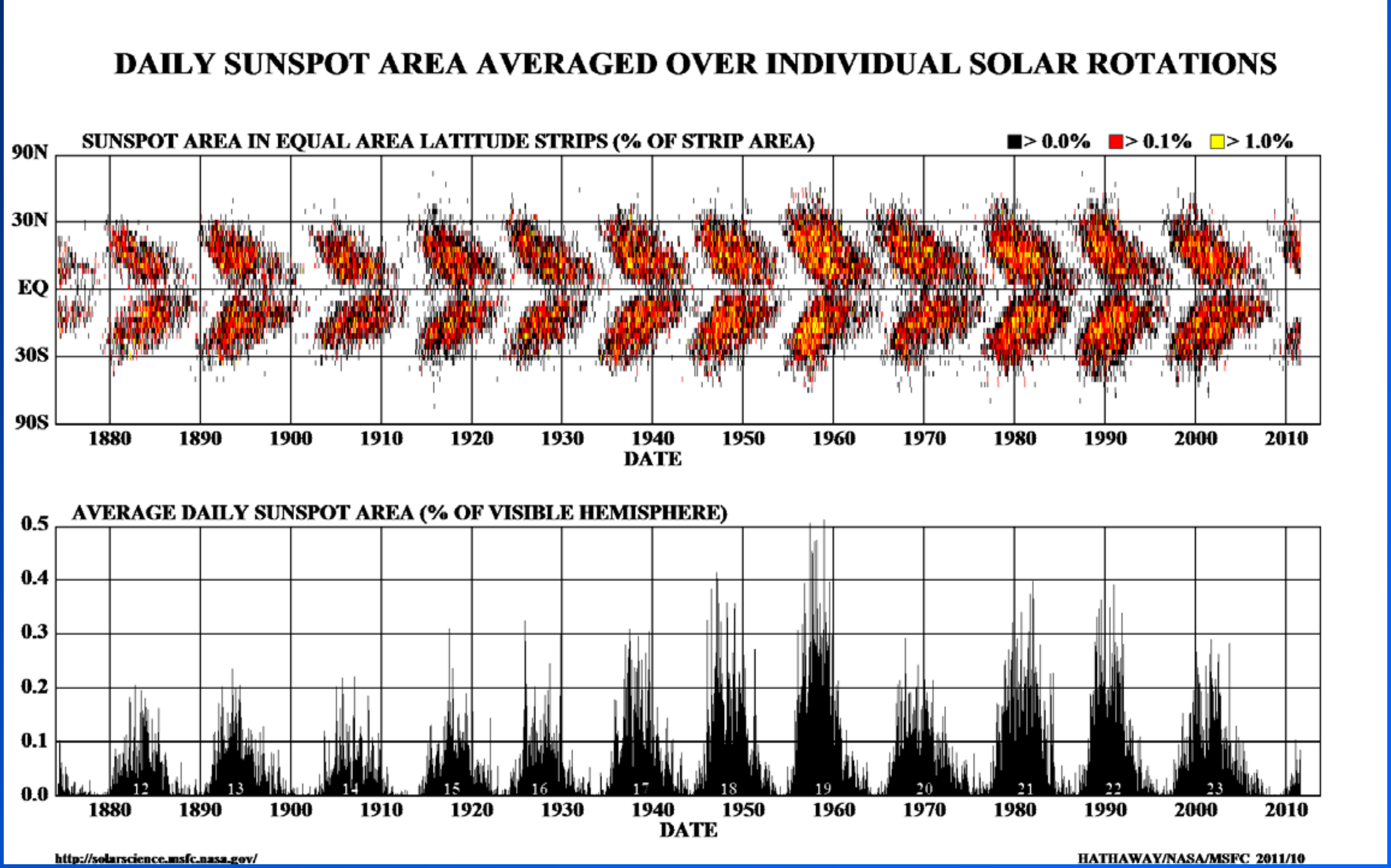

Hale's Law

In 1919 Hale (along with Ellerman, Nicholson, and Joy) found that the magnetic field in sunspots followed a definite law, "Hale's Law" such that: *"…the preceding and following spots … are of opposite polarity, and that the corresponding spots of such groups in the Northern and Southern hemispheres are also opposite in sign. Furthermore, the spots of the present cycle are opposite in polarity to those of the last cycle".*

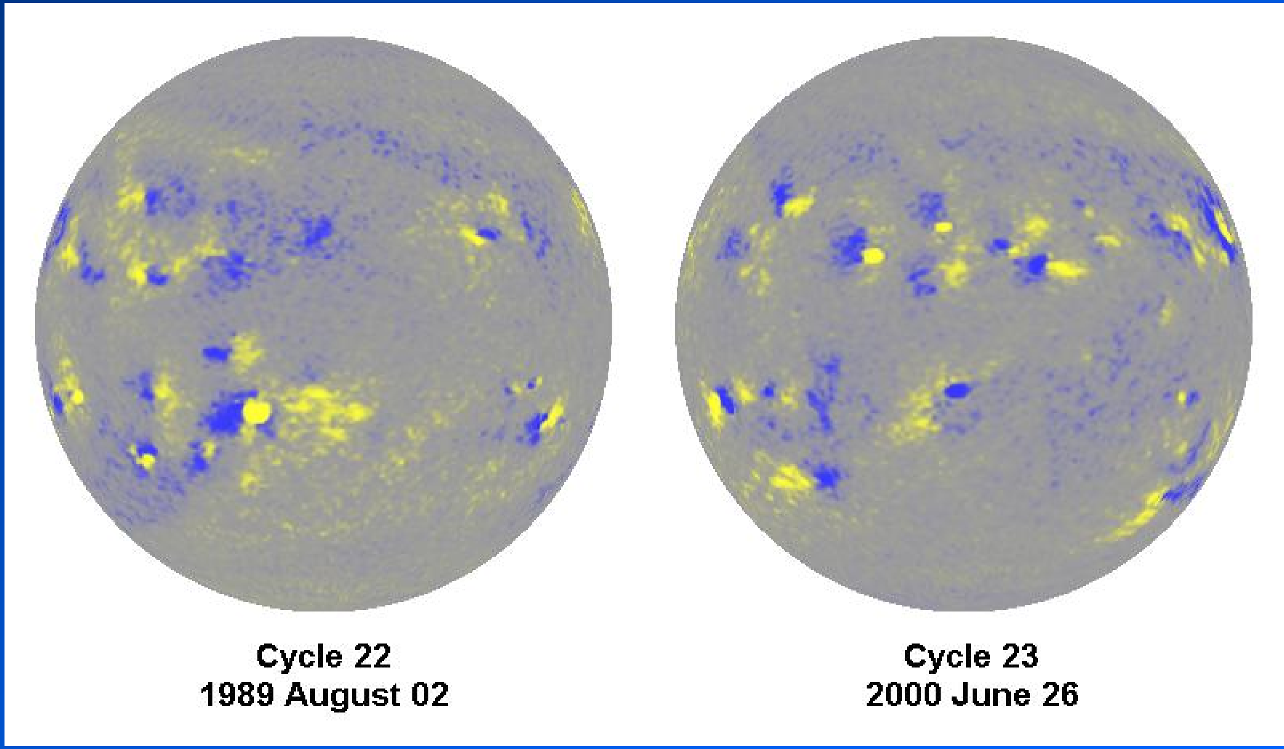

Joy's Law

In that 1919 paper Joy noted that sunspot groups are tilted with the leading spots closer to the equator than the following spots. This tilt increases with latitude.

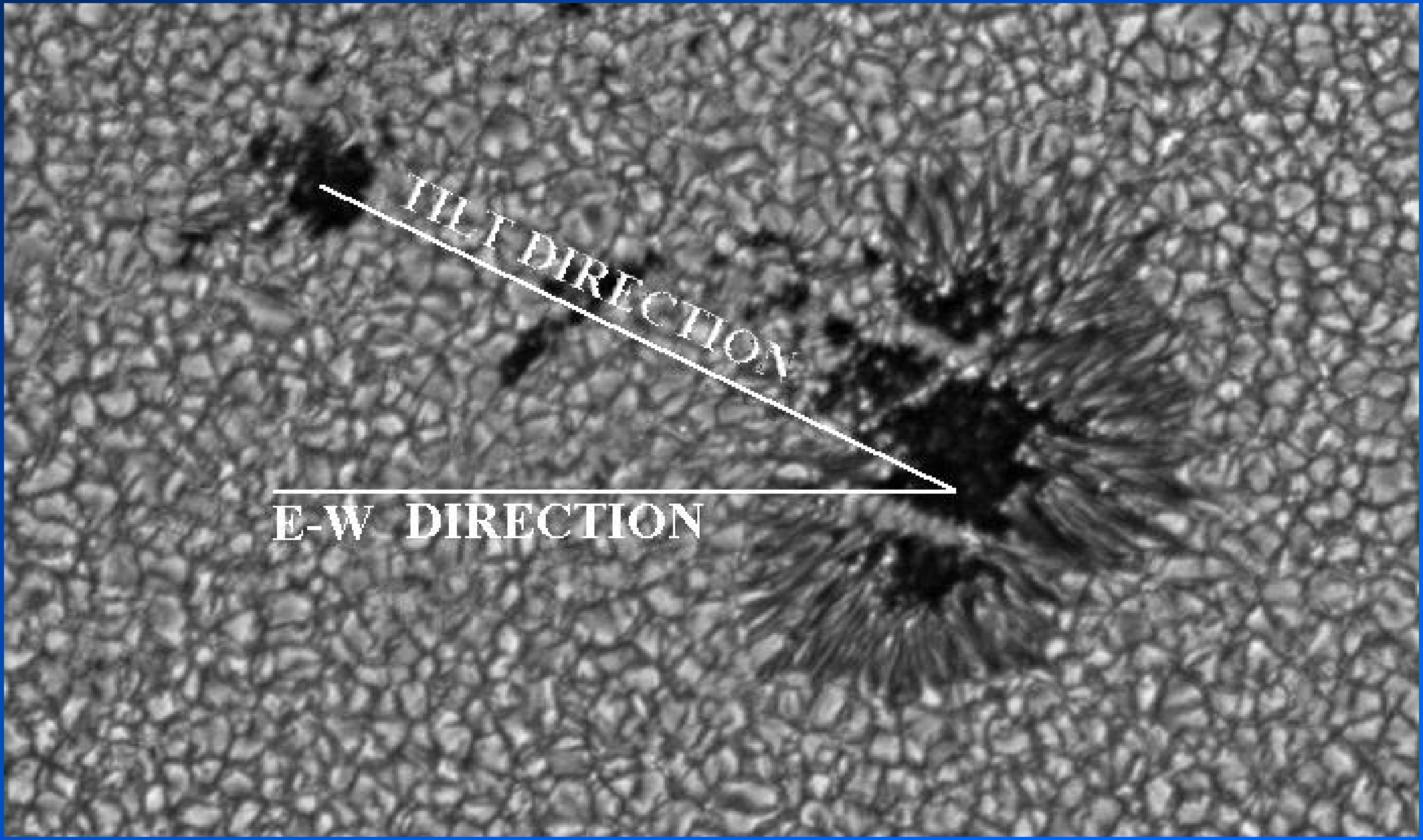

The Solar Cycle in 3D

In addition to these magnetic polarity changes and the equatorward drift of the sunspot latitudes, there are important flows on the surface and within the Sun: *Differential Rotation* – faster at the equator, slower near the poles; and *Meridional Flow* – flow from the equator toward the poles along the surface.

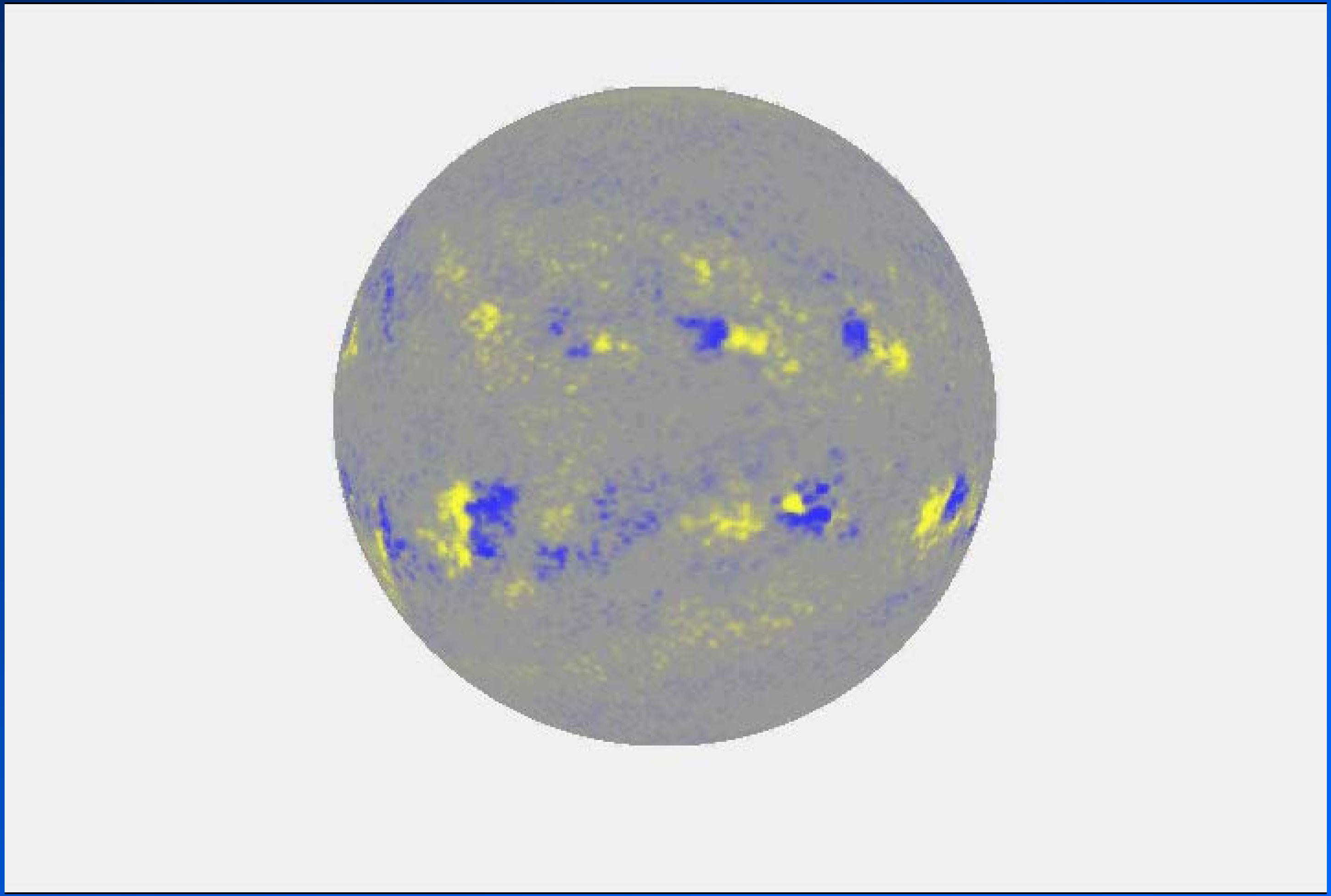

Supergranule Diffusion

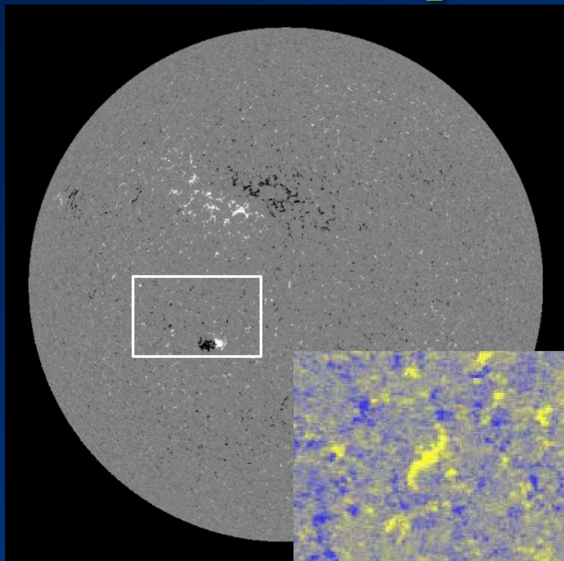

Convective motions (supergranules) carry magnetic elements to their evolving boundaries in a diffusion-like random walk.

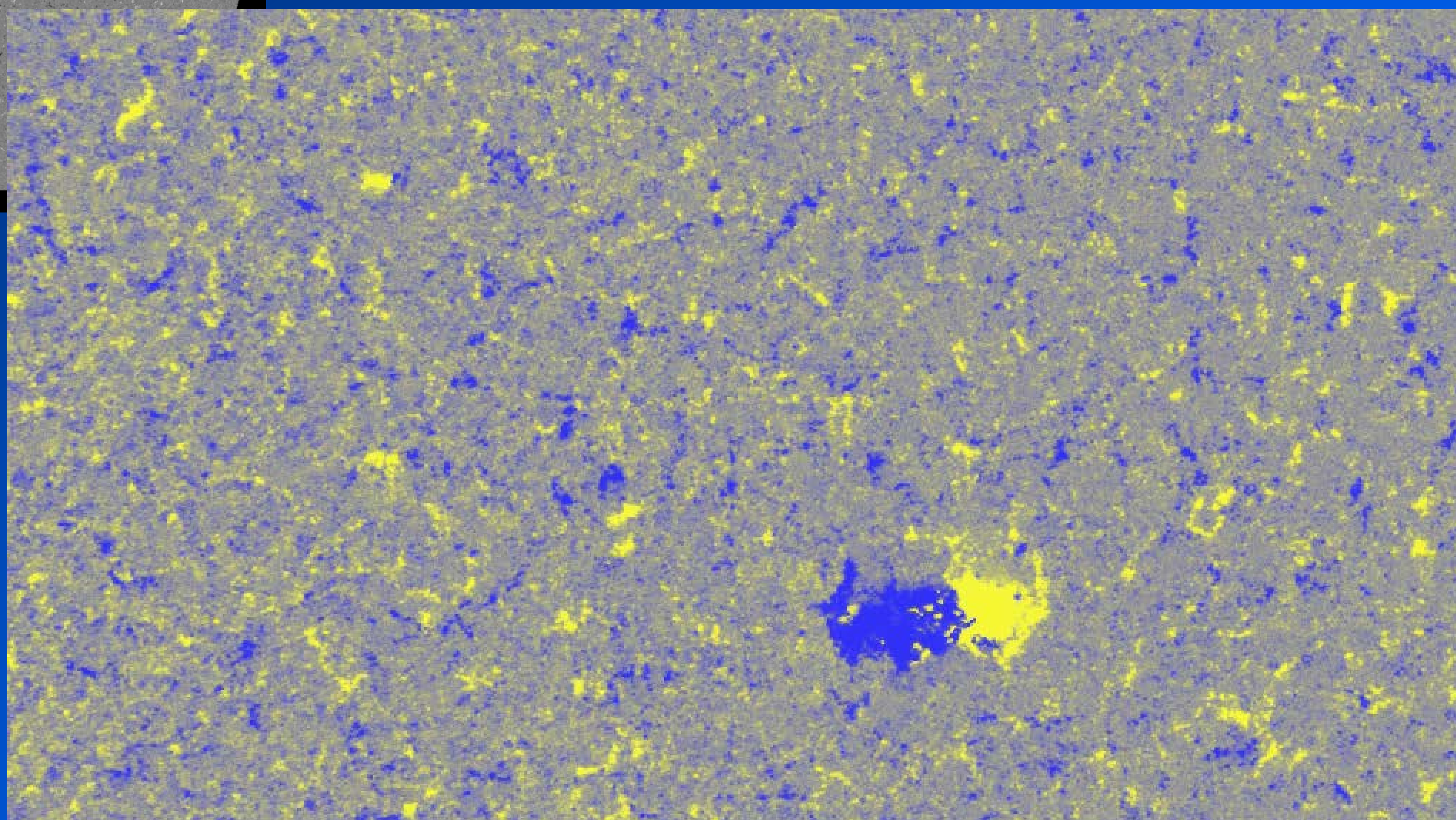

Polar Field Reversals

In 1958 Harold Babcock and Bill Livingston noted that the magnetic polarities of the Sun's weak polar fields also reverse from one cycle to the next, and that this reversal happens at about the time of sunspot cycle maximum.

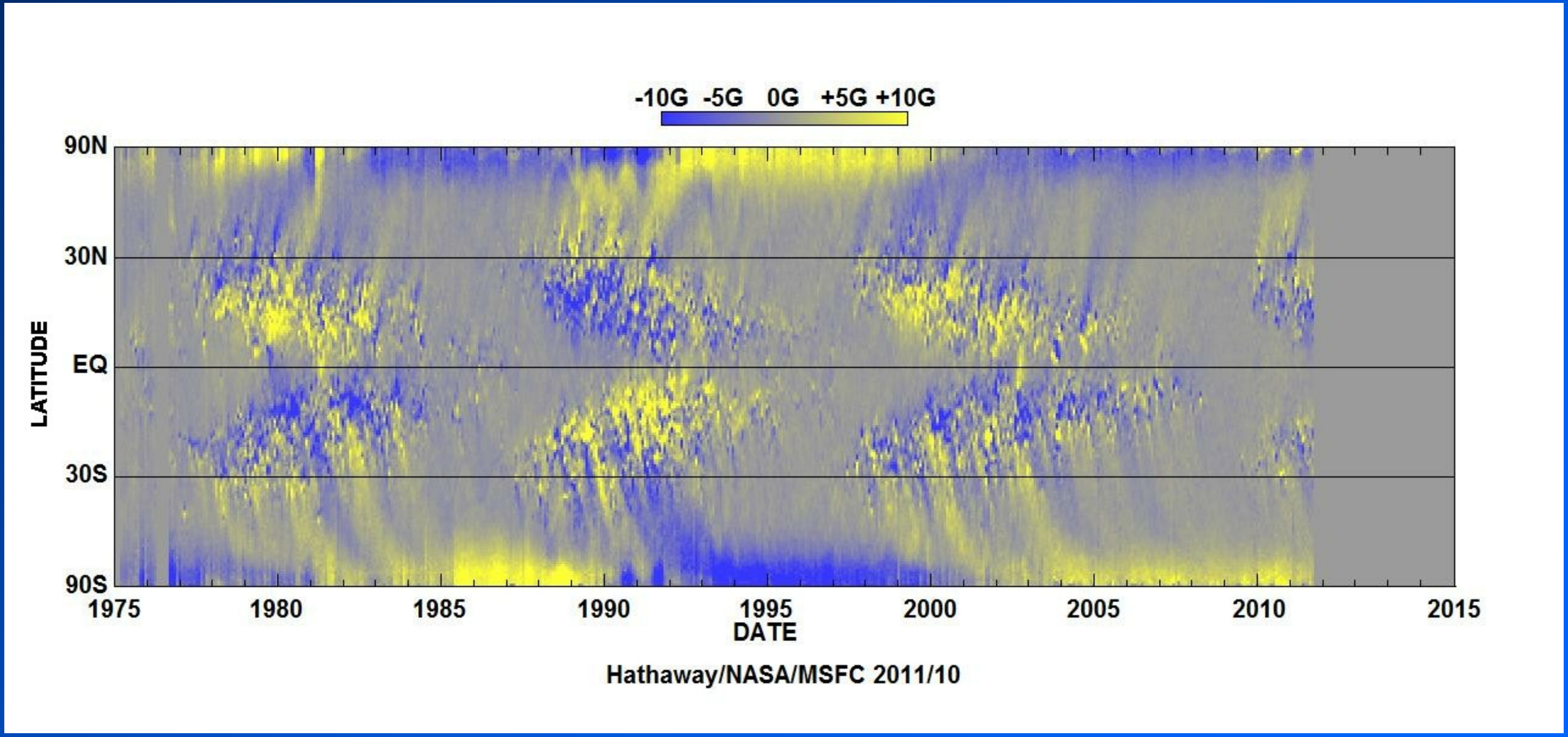

The dominant magnetic polarity on the poleward sides of these zones is carried toward the poles where it reverses the old cycle polarity.

The Solar Dynamo Saga

The first 100 years

Anti-Dynamo to Dynamo

1908 – Hale discovers magnetic fields in sunspots

1913 – Hale, Ellerman, Nicholson, & Joy find Hale's Law and Joy's Law

1919 – Larmor suggests that the Sun's magnetic fields could be produced by the motions of an electrically conducting fluid in a rotating body

1934 – Cowling shows that a steady axisymmetric field cannot be maintained by axisymmetric flows - "Anti-Dynamo Theorem"

1945 - Cowling calculates a decay time for "fossil" field (10^{10} years) incompatible with 11-year cycle – must have dynamo activity.

1946 – Elsasser initiated the use of non-axisymmetric flows

1954 – Bullard & Gellman recognize the need for two ingredients – differential rotation and non-axisymmetric lifting and twisting

Solar Dynamo Basics

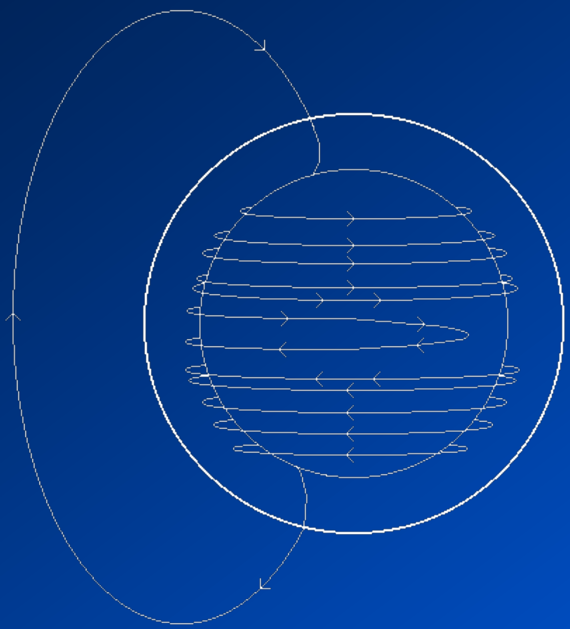

Two processes are common to nearly all solar dynamos-

Differential rotation (rotational shear in either latitude or radius) stretches out (poloidal) field lines in the longitudinal (toroidal) direction – **The Omega Effect**

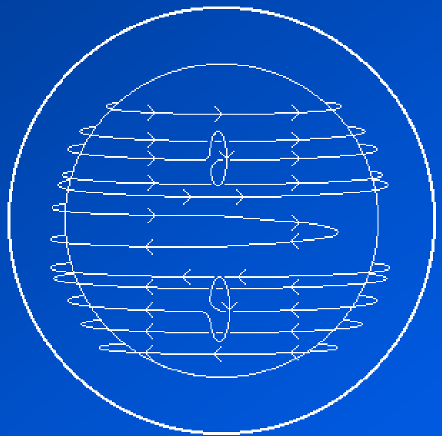

Lifting and twisting of these field lines by non-axisymmetric motions takes the intensified longitudinal (toroidal) fields and rotates them back into meridional (poloidal) direction – **The Alpha Effect**

Babcock (1961)

(son Horace , not father Harold)

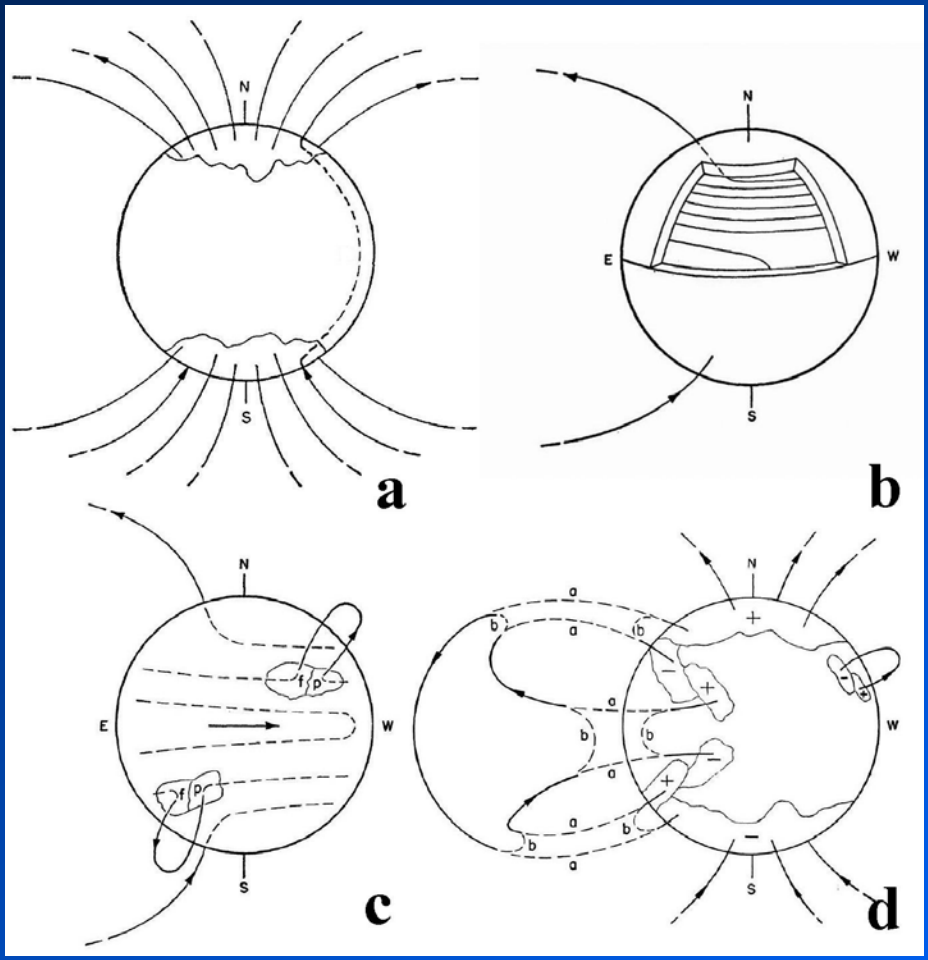

a) Dipolar field at cycle minimum threads through a shallow layer below the surface.

b) Latitudinal differential rotation shears out this poloidal field to produce a strong toroidal field (first at the mid-latitudes then progressively lower latitudes).

c) Buoyant fields erupt through the photosphere giving Hale's polarity law and Joy's Tilt.

d) Meridional flow away from the active latitudes gives reconnection at the poles and equator.

Leighton (1969)

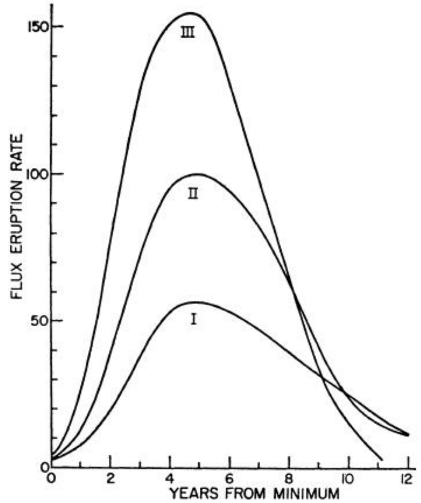

FIG. 9.—The development of a cycle as a function of average maximum amplitude. I, II, III refer respectively to the lowest, middle, and highest thirds of the cycles, in terms of the maximum amplitude attained.

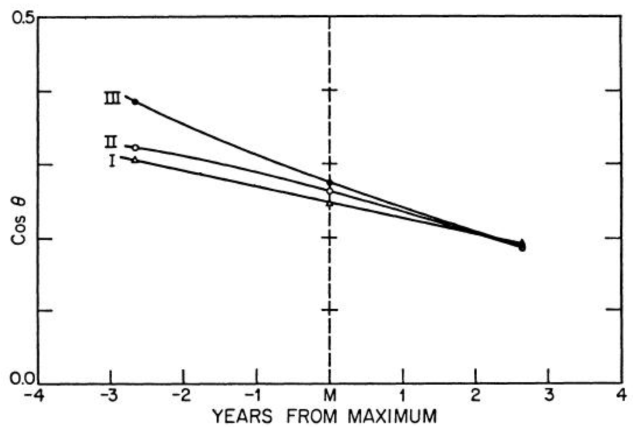

FIG. 10.—Dependence of the latitude variation of the sunspot zone on the maximum amplitude of a cycle. I, II, III refer to the same groups of cycles as in the previous figure.

- Supergranules (which were "discovered" by Leighton, Noyes, & Simon in 1962) provide diffusive transport of 10^4 km^2/s in the photosphere (no meridional flow as in Babcock's model).

- A rotation rate increasing inward is required for equatorward drift of the active latitudes.

- A numerical model for the depth and longitude averaged magnetic field reproduced many observed aspects – provided several adjustable parameters are set.

Mean Field Theory

HIROKAZU YOSHIMURA

II. BASIC EQUATIONS AND METHODS

The magnetohydrodynamic equations for the mean magnetic field of the medium, in which velocity and magnetic fields of smaller scale prevail, differ from the usual MHD equations in the appearance of a new term in the induction equation (Steenbeck, Krause, and Rädler 1966; Steenbeck and Krause 1966; Rädler 1968; Braginskii 1964*a*, *b*). That is, if we separate the velocity and magnetic fields of the continuous medium $\boldsymbol{V}$, $\boldsymbol{H}$ into the mean fields $\langle \boldsymbol{V} \rangle$, $\langle \boldsymbol{H} \rangle$ and perturbed fields $\boldsymbol{v}$, $\boldsymbol{h}$, i.e., $\boldsymbol{V} = \langle \boldsymbol{V} \rangle + \boldsymbol{v}$, $\boldsymbol{H} = \langle \boldsymbol{H} \rangle + \boldsymbol{h}$, then the equations governing the mean magnetic field are given by

$$\frac{\partial \langle \boldsymbol{H} \rangle}{\partial t} = \nabla \times (\langle \boldsymbol{V} \rangle \times \langle \boldsymbol{H} \rangle) + \nabla \times \langle \boldsymbol{v} \times \boldsymbol{h} \rangle - \eta_m \nabla \times (\nabla \times \langle \boldsymbol{H} \rangle) , \tag{2.1}$$

$$\nabla \cdot \langle \boldsymbol{H} \rangle = 0 , \tag{2.2}$$

where the angular brackets indicate mean fields obtained by some averaging process and the dissipation term is assumed to be described by internal, uniform, and isotropic magnetic diffusivity η_m. The term $\nabla \times \langle \boldsymbol{v} \times \boldsymbol{h} \rangle$ represents the action of the smaller-scale fields on the mean magnetic field, and it may work as a dissipation mechanism and/or as a dynamo mechanism.

αΩ Dynamos

THE GENERATION OF MAGNETIC FIELDS IN ASTROPHYSICAL BODIES. I. THE DYNAMO EQUATIONS

E. N. PARKER
Department of Physics, University of Chicago
Received 1970 April 6; revised 1970 May 15

ABSTRACT

The paper presents a formal derivation of the dynamo equations describing the generation of large-scale magnetic fields by small-scale cyclonic turbulence (or convection) in a rotating fluid body. The derivation is based on the simple approximation that the individual turbulent cells are small and short-lived.

The dynamo equations show that large-scale magnetic fields are generated at a very high rate, in periods comparable to the time of nonuniform rotation. The dynamo equations describe the generation of the quasi-steady field of Earth and the migratory field of the Sun, in characteristic times of 10^3 and 10 years, respectively.

I. INTRODUCTION

Elsasser (1945, 1946, 1947, 1950) and Bullard (1949) pointed out that the nonuniform rotation $V_\phi(\varpi, z)$ in the liquid metal core of Earth draws out the lines of force of the geomagnetic dipole field to form a strong azimuthal field. The generation of azimuthal field from the poloidal dipole field is described by the familiar hydromagnetic equation

$$\left(\frac{\partial}{\partial t} - \eta\nabla^2\right) B_\phi = e_\phi\left[B_z \frac{\partial V_\phi}{\partial z} + B_\varpi\left(\frac{\partial V_\phi}{\partial \varpi} - \frac{V_\phi}{\varpi}\right)\right] \qquad (1)$$

in cylindrical coordinates (ϖ, ϕ, z), where η is the resistive diffusivity ($\eta = c^2/4\pi\sigma$ if σ is in esu; $\eta \simeq 10^5\ \mathrm{cm^2\ sec^{-1}}$ for the liquid iron core of Earth and $\simeq 10^9\ \mathrm{cm^2\ sec^{-1}}$ in the solar photosphere). Some years later we pointed out (Parker 1955) that the dipole field B_ϖ, B_z is generated from the azimuthal field B_ϕ by the convection or turbulence in the rotating fluid body. The mechanism is simple. The Coriolis forces on the convection cause it to be cyclonic, with a rising cell of fluid rotating and carrying the lines of force of the azimuthal field into loops with nonvanishing projection on the meridional plane (see schematic drawing, Fig. 1). A large number of such loops coalesce to regenerate the dipole field. In the approximation that the nonuniform rotation is strong and that there are many short-lived small-scale cyclonic convective cells, the generation of poloidal field is described by the dynamo equation

$$\left(\frac{\partial}{\partial t} - \eta\nabla^2\right) A_\phi = \Gamma(r, t) B_\phi\,, \qquad (2)$$

- Toroidal field, B_ϕ, is generated from poloidal field by the Omega effect – shearing by differential rotation - $\nabla\Omega$.

- Poloidal field, $\nabla\times A_\phi$, is generated from toroidal field by the alpha effect – cyclonic flows – $\alpha \sim v\cdot\nabla\times v$.

- A dynamo wave travels along isorotation surfaces with frequency $\sim \sqrt{\alpha\nabla\Omega}$

Dynamo Dilemma #1

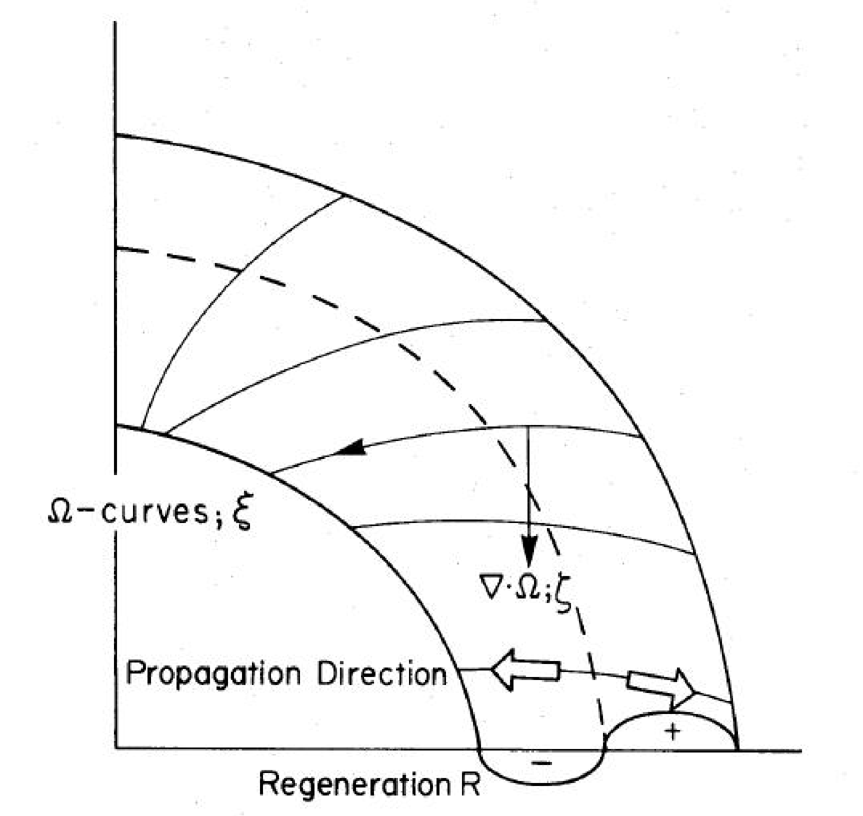

While equatorward propagation could be achieved if the rotation rate increased inward across the convection zone, **the α-effect in the bulk of the convection zone is orders of magnitude too large** and gives short period (2-year instead of 22-year) dynamos no matter how the internal rotation rate varies.

3D-MHD Dynamos

• **Gilman & Miller (1981) "Dynamically consistent nonlinear dynamos driven by convection in a rotation spherical shell"**

• **Glatzmeier (1985) "Numerical simulations of stellar convective dynamos. II. Field propagation in the convection zone"**

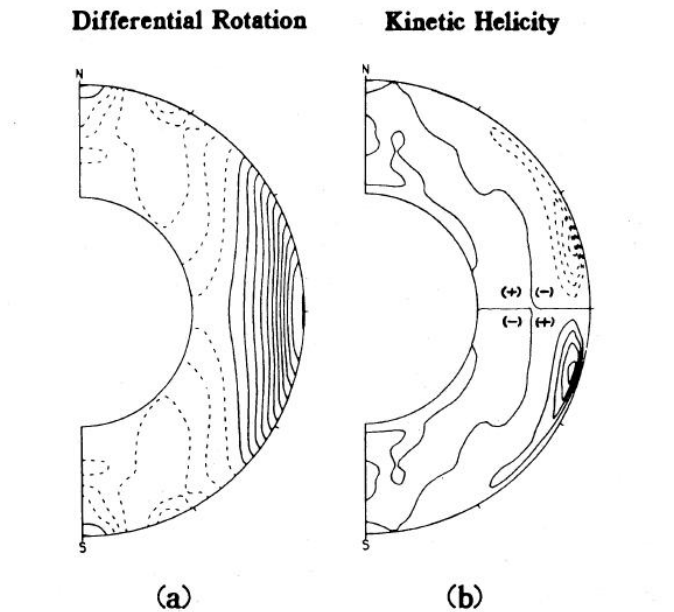

FIG. 2.—(*a*) Solid (broken) contours represent positive (negative) angular velocity relative to the rotating frame of reference. (*b*) Solid (broken) contours represent positive (negative) helicity averaged longitude.

This was the original Anelastic Spherical Harmonic (ASH) code with ℓ_{max}=19.

Oscillatory dynamos were produced but the dynamo waves moved poleward and the periods were too short by an order of magnitude.

Dynamo Dilemma #2

The toroidal magnetic flux produced in the convection zone should be buoyant and rise rapidly (weeks) to the surface (Parker, 1975). This short residence time would not allow the Ω-effect to intensify the field enough.

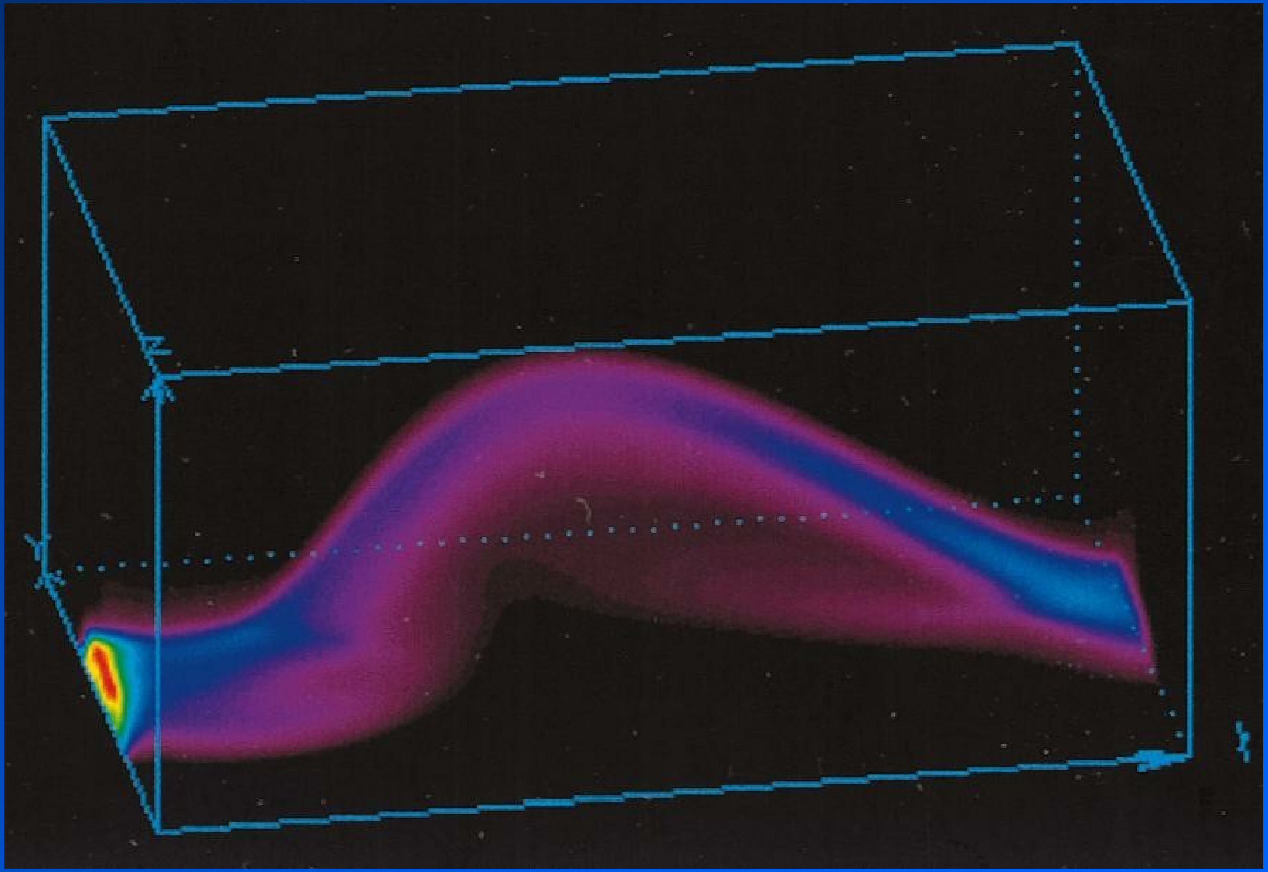

Abbett, Fisher & Fan (2001)

Dynamo Dilemma #3

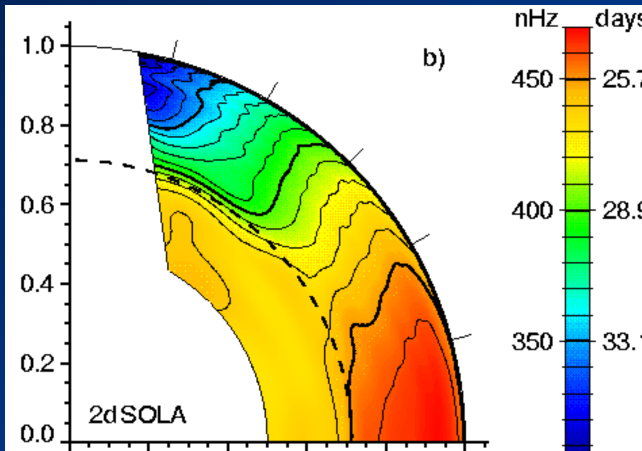

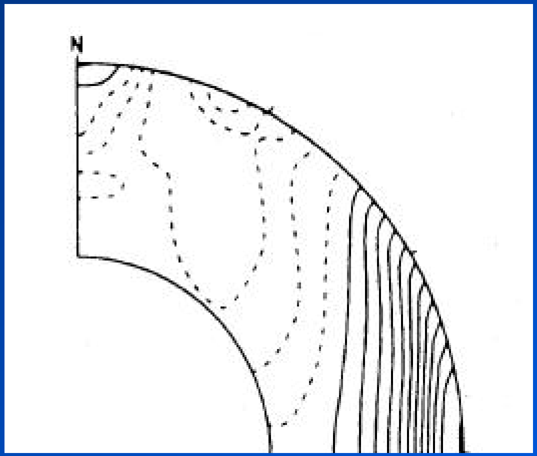

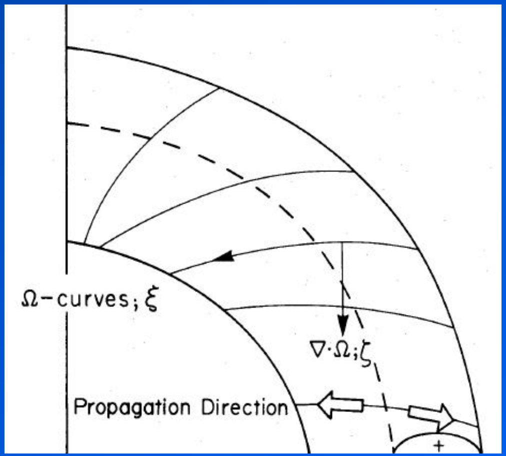

Observed (Helioseismology) **Hydrodynamic Model** **Kinematic Model**

The internal rotation profile determined with helioseismic methods shows shear layers at the top and bottom of the convection zone with nearly constant rotation rate in between – unlike the rotation profiles produced in the hydrodynamic models or assumed in the kinematic dynamo models.

Solution: Interface Dynamos

All three dilemmas (too much α-effect, buoyant flux tube rise time, and wrong radial shear) could be circumvented if the dynamo was placed at the base of the convection zone.

Parker (1975) made this suggestion early on to solve the magnetic buoyancy dilemma.

DeLuca & Gilman (1986) produced dynamo models in which the overshooting convective motion act on the magnetic field and could produce longer period dynamo oscillations.

The dynamics of flux tubes rising rapidly through a rotating convection zone dramatically reduces the twisting otherwise produced by the convection itself.

Interface Dynamo Waves

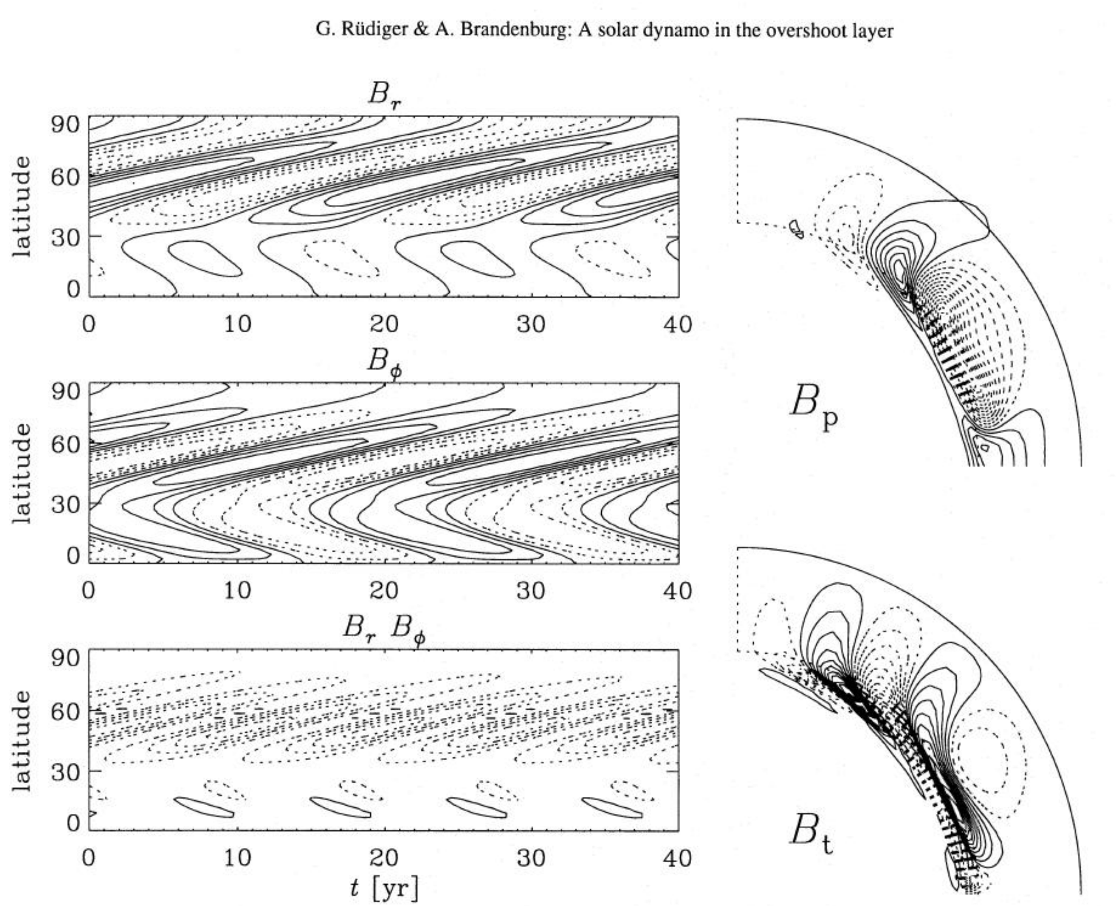

Fig. 6. The magnetic field geometry for the nonlinear (α-quenched) solution with buoyancy and $\epsilon = 0.5$, $d = 0.05R$, $\alpha_U = 1$

The shear layer at the base of the convection zone has rotation rate decreasing inward at latitudes below about 30º and increasing inward at higher latitudes.

This gives two dynamo waves – one moving toward the equator below 30º and another moving poleward at higher latitudes.

Dynamo Dilemma #4

The poleward branch due to the high-latitude shear at the base of the convection zone is not observed.

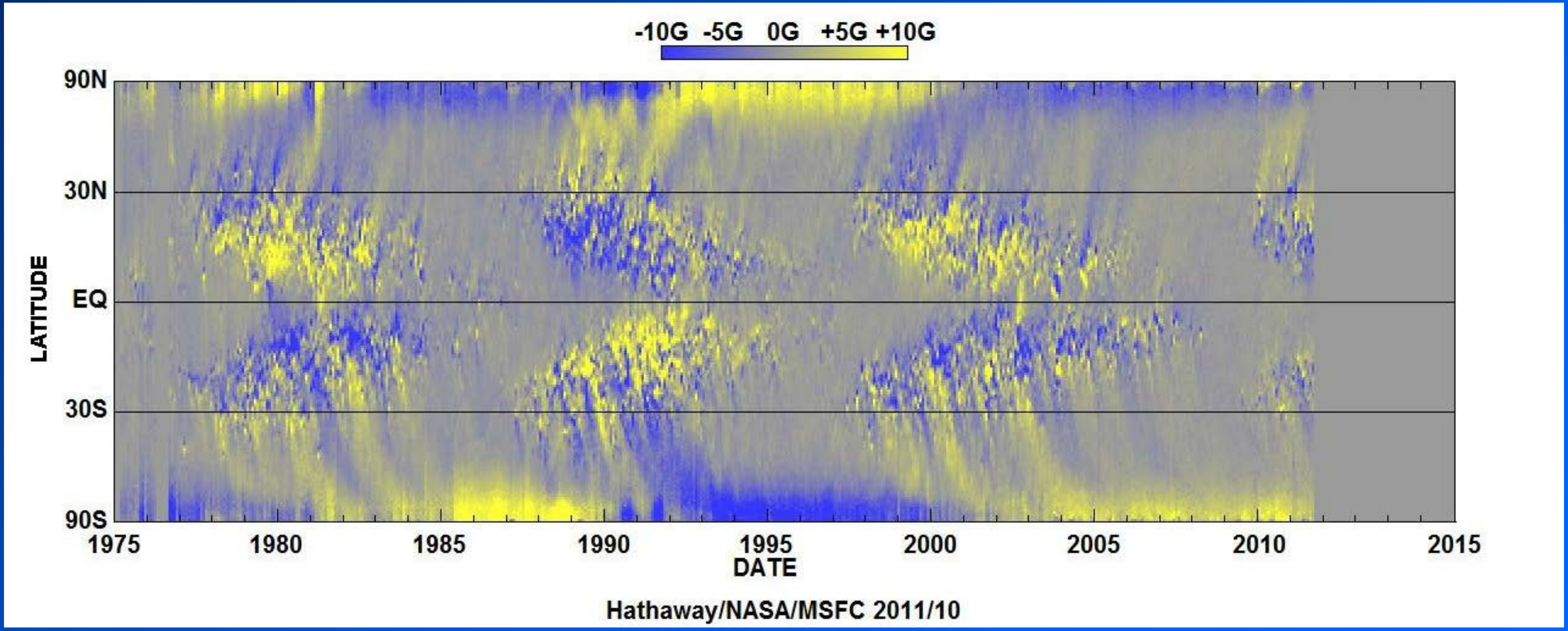

Solution: Deep Meridional Flow

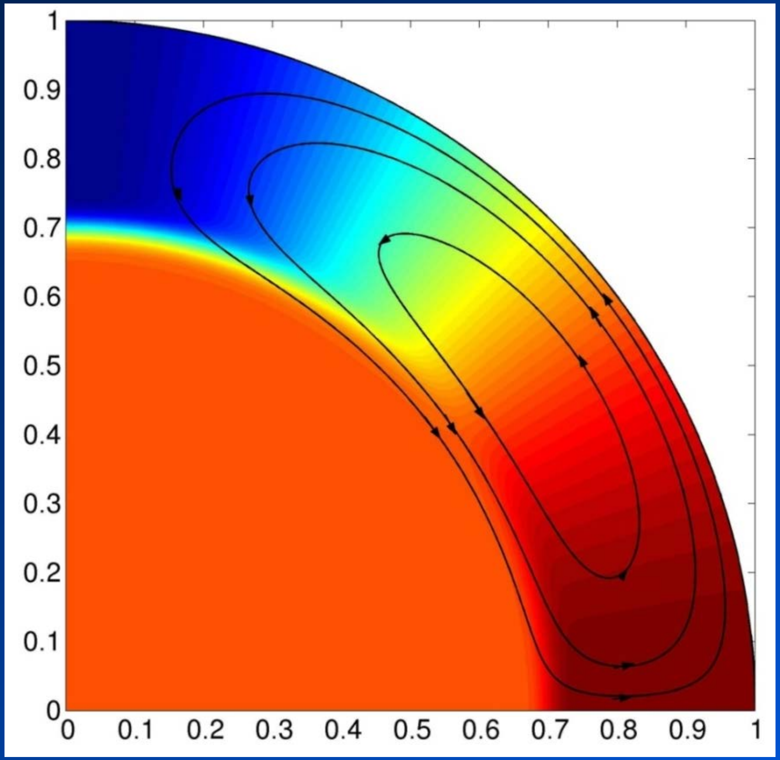

Nandy & Choudhuri (2002)

Dikpati & Choudhuri (1994, 1995) proposed Flux Transport Dynamos which produced only equatorward drifting activity zones by assuming that the poleward meridional flow seen at the surface turns equatorward midway through the convection zone which could produce a return flow velocity of 1-2 m/s at the base of the convection zone.

In these models the return flow at the base of the convection zone gives the 1-2 m/s equatorward drift of the active latitudes and the 22-year period of the magnetic cycle.

A Flux Transport Dynamo

Dikpati & Charbonneau (1999) investigated the characteristics of these dynamos and their sensitivity to changes in flow parameters. The meridional flow speed controls both the dynamo period and its strength.

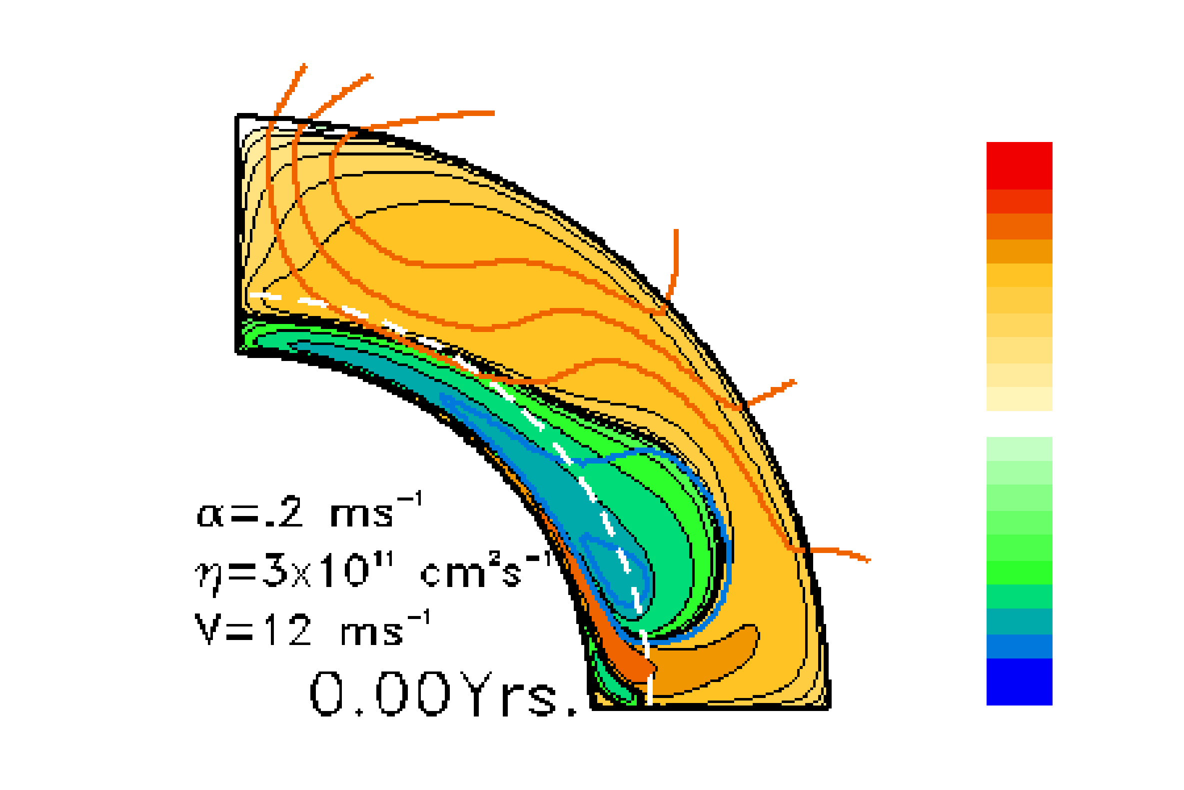

In/CCW

Out/CW

Chapter 11:

Why Flux Transport Dynamos are Bankrupt

Dikpati Dynamo Prediction

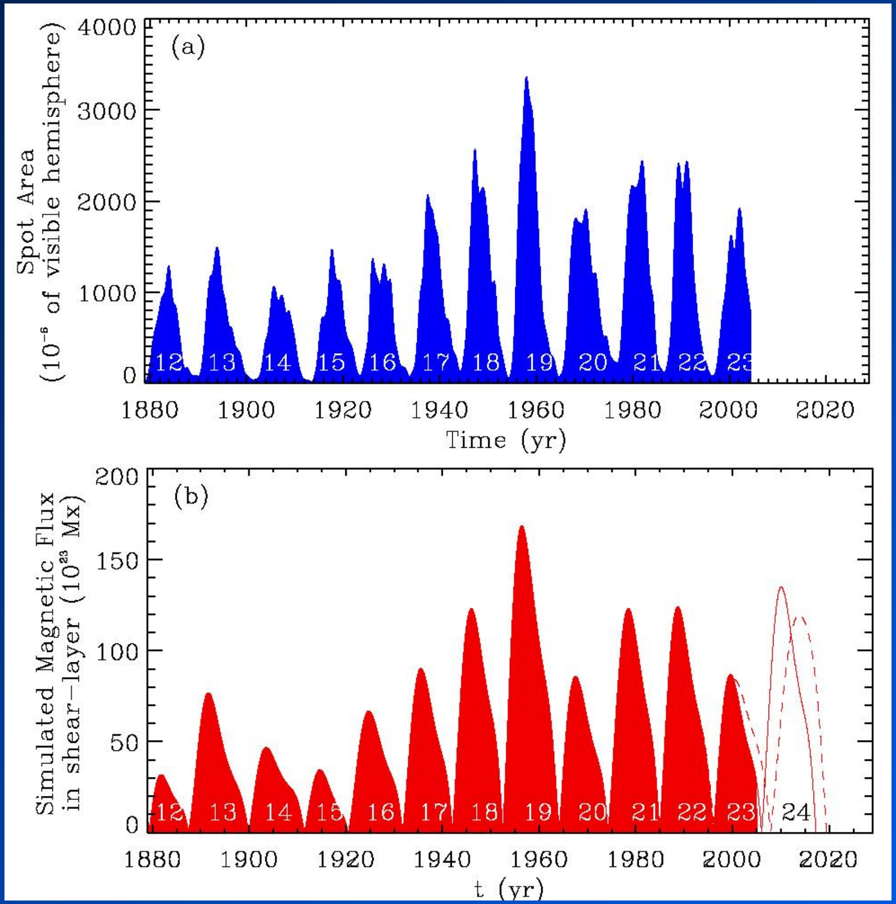

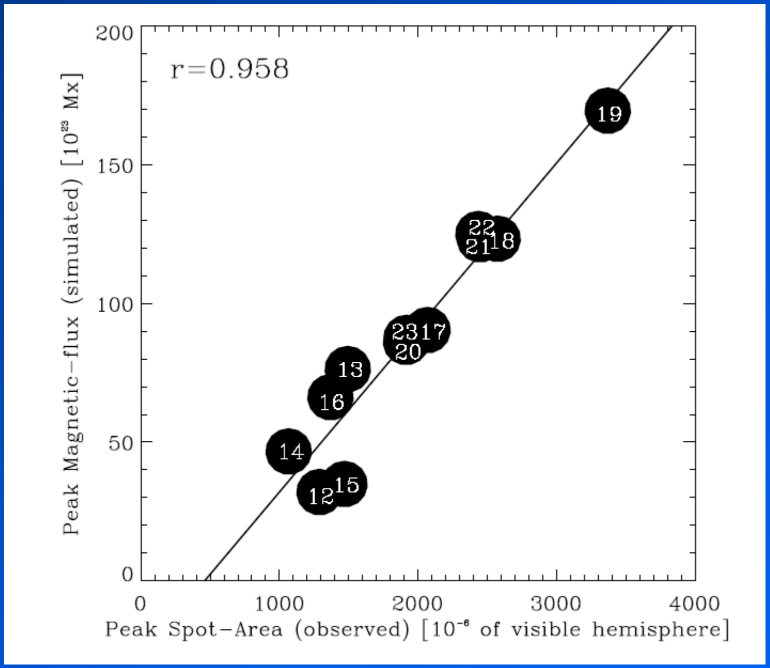

Cycle 24 Prediction ~ 180 ± 15
(with slow flow: late and ~ 165 ± 15

Dikpati, de Toma & Gilman (2006) fed sunspot areas and positions into their numerical model for the Sun's dynamo and reproduced the amplitudes of the last eight cycles with unprecedented accuracy (RMS error < 10).

Indications of Problems

1. They used my data for sunspot areas – which were 20% high for cycle 20. Their prediction for cycle 20 fit the erroneous value and later cycles were also predicted accurately in spite of the error in the input data. (They later ran the prediction again with the corrected values and found that the predictions didn't change too much.)

2. They kept the meridional flow speed constant. Yet, they allow it to slow in cycle 23 and find a 10% drop in the prediction. Similar variations in meridional flow speed should have occurred in the past.

Measuring Axisymmetric Flows

Hathaway & Rightmire (*Science* 327, 1350, 2010; *ApJ* 729, 80, 2011) cross-correlated the features in strips from 60,000 magnetic maps of the Sun obtained at a 96-minute cadence from 1996 to 2011 to determine the axisymmetric flow components for each solar rotation.

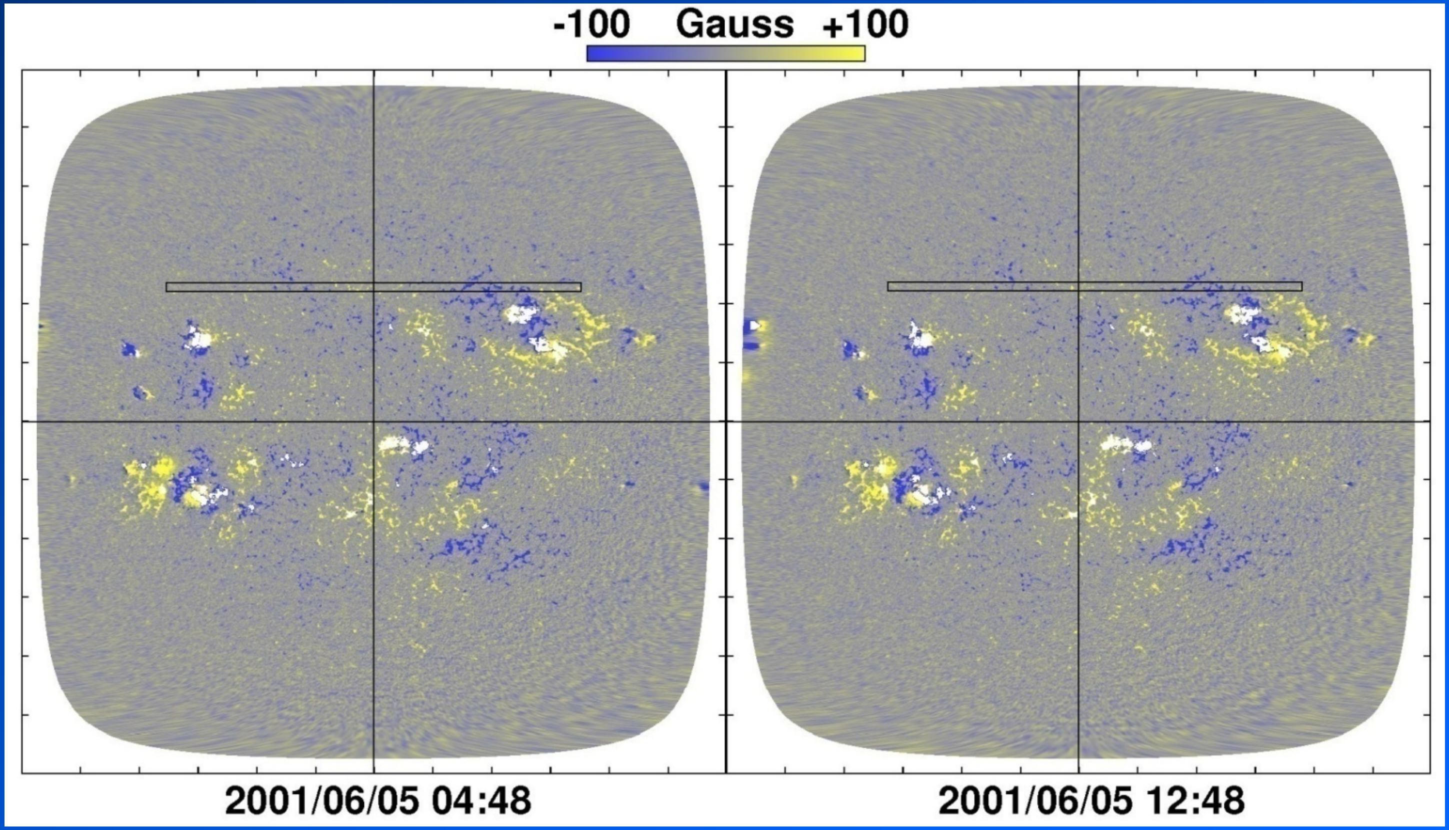

Axisymmetric Flow Profiles

Our MDI data included corrections for CCD misalignment, image offset, and a 150 year old error in the inclination of the ecliptic to the Sun’s equator. We extracted differential rotation and meridional flow profiles from over 60,000 image pairs from May of 1996 to September of 2010.

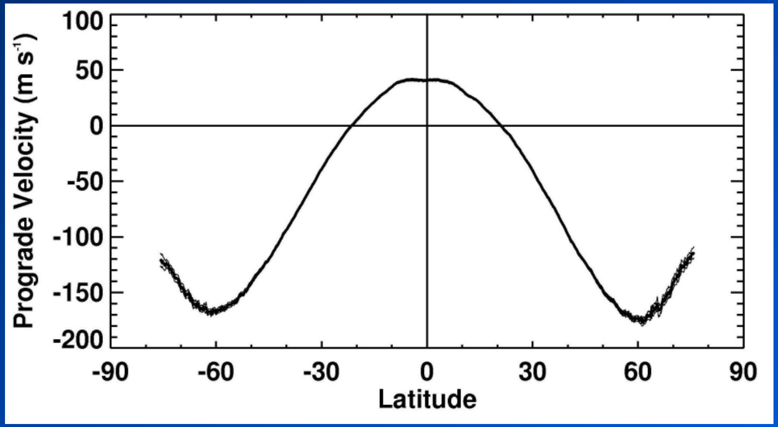

Average (1996-2010) differential rotation profile with 2σ error limits.

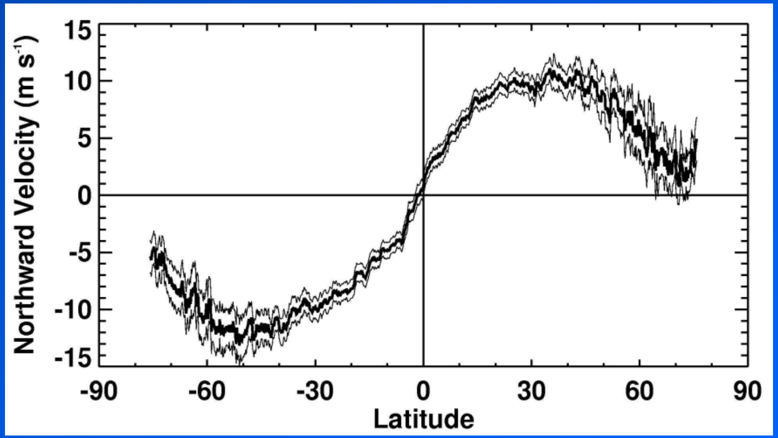

Average (1996-2010) meridional flow profile with 2σ error limits.

Solar Cycle Variations in Flow Amplitude

While the differential rotation does vary slightly over the solar cycle, it is the meridional flow that shows the most significant variation. The Meridional Flow slowed from 1996 to 2001 but then increased in speed again after maximum. The slowing of the meridional flow at maximum seems to be a regular solar cycle occurrence (Komm, Howard, & Harvey, 1993). The greater speed up after maximum is specific to Cycle 23.

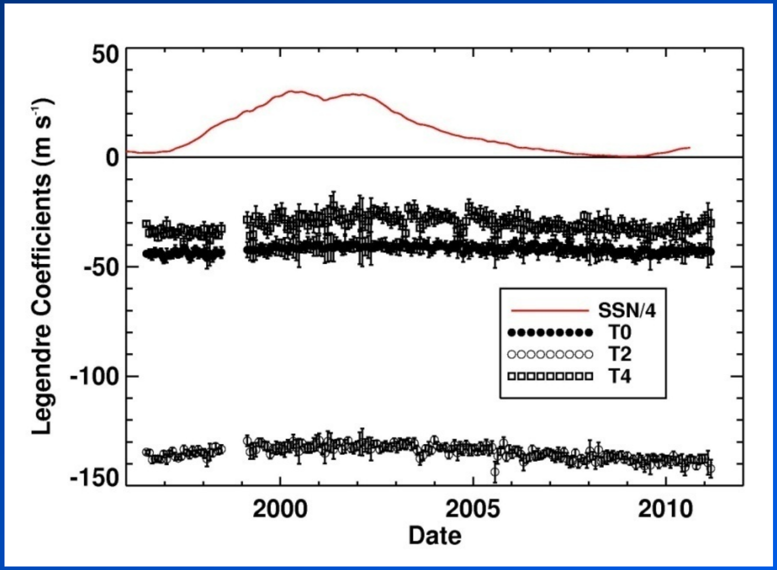

Differential rotation variations

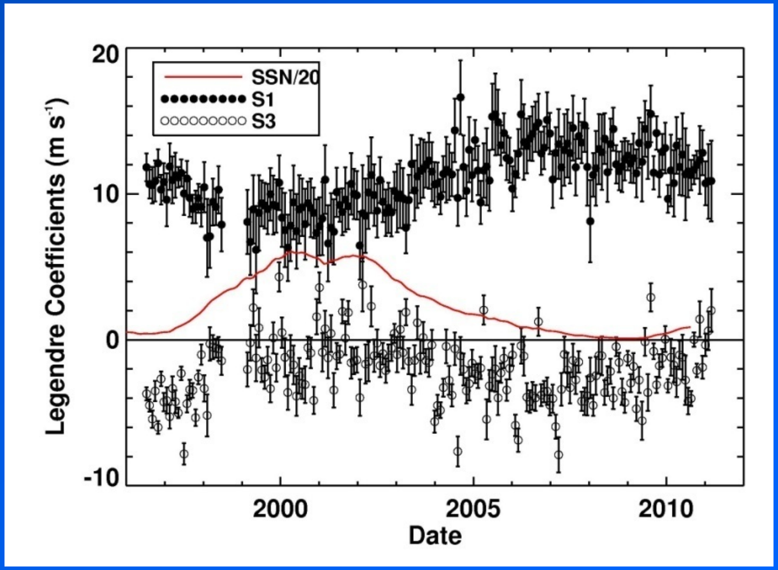

Meridional flow variations

Solar Cycle Variations in Flow Structure

The differential rotation and meridional flow profiles for each solar rotation also show that the differential rotation changes very little while the meridional flow changes substantially (and includes countercells with equatorward flow near the south pole early and the north pole later).

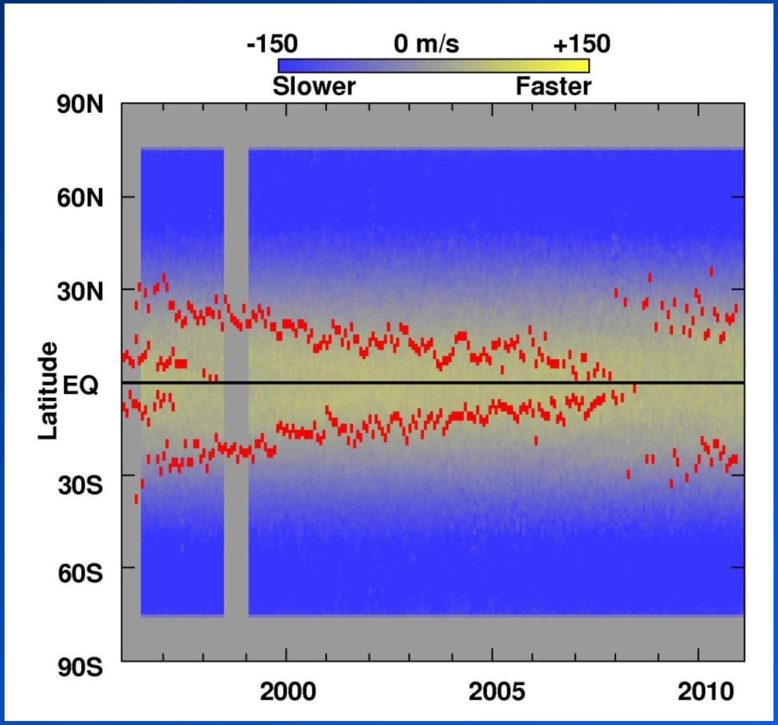

Differential rotation profiles

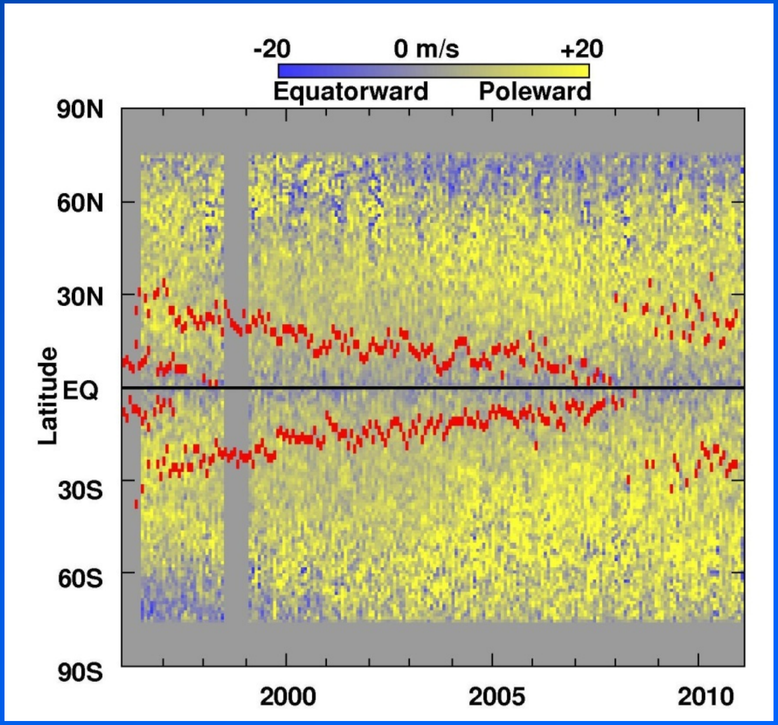

Meridional flow profiles

Differences from Average

Removing the average, symmetric profiles reveals the torsional oscillations (faster rotation on the equatorward side of the sunspot latitudes and slower poleward with faster polar rotation at maximum) and a system of inflows toward the sunspot latitudes. The equatorward inflow at higher latitudes is identified as the source of the slower meridional flow at cycle maxima.

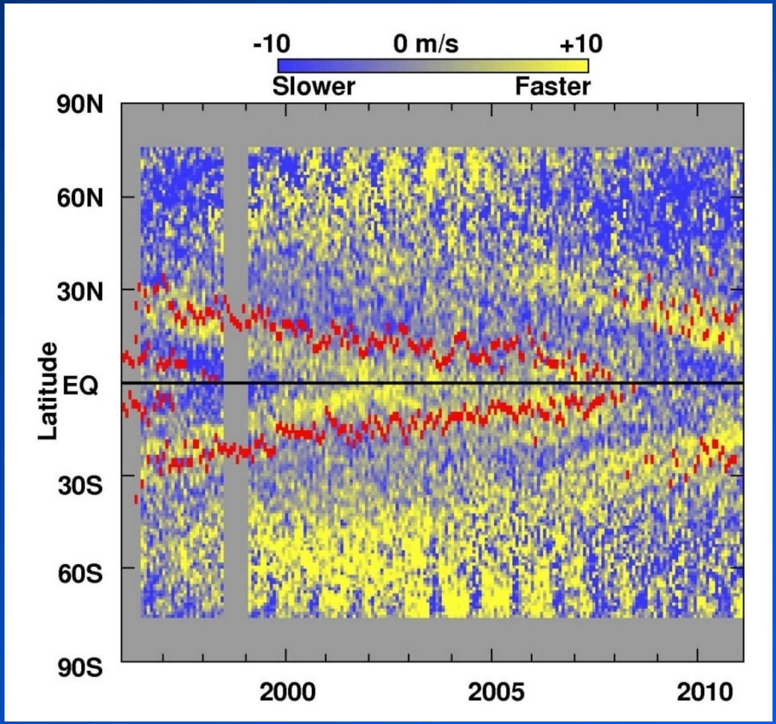

Differential Rotation

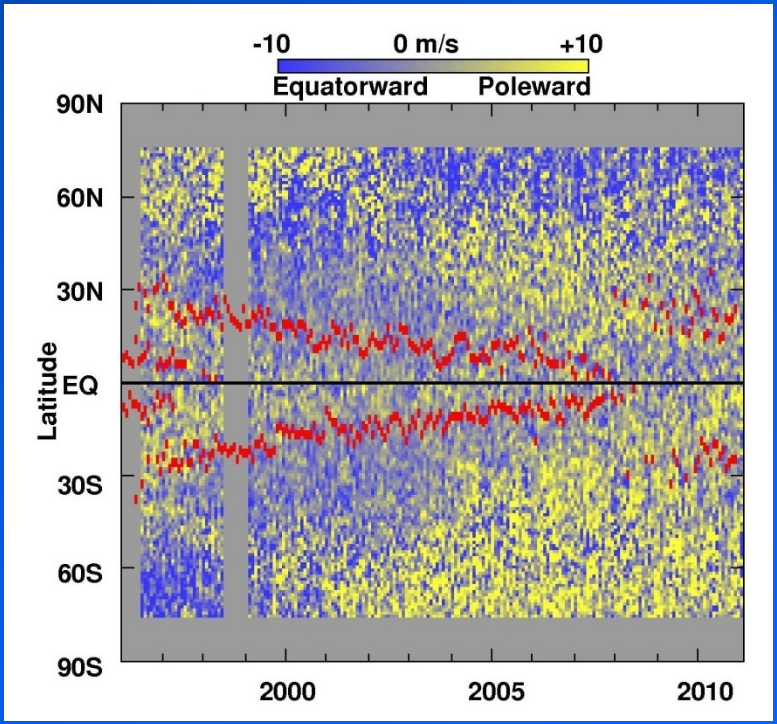

Meridional Flow

Nandy et al. (2011)

Nandy et al. *Nature* 471, 80 (2011) showed that they could reproduce the weak polar fields and long period of Cycle 23 in their Flux Transport Dynamo if the meridional flow was fast during the first half and slow during the second half.

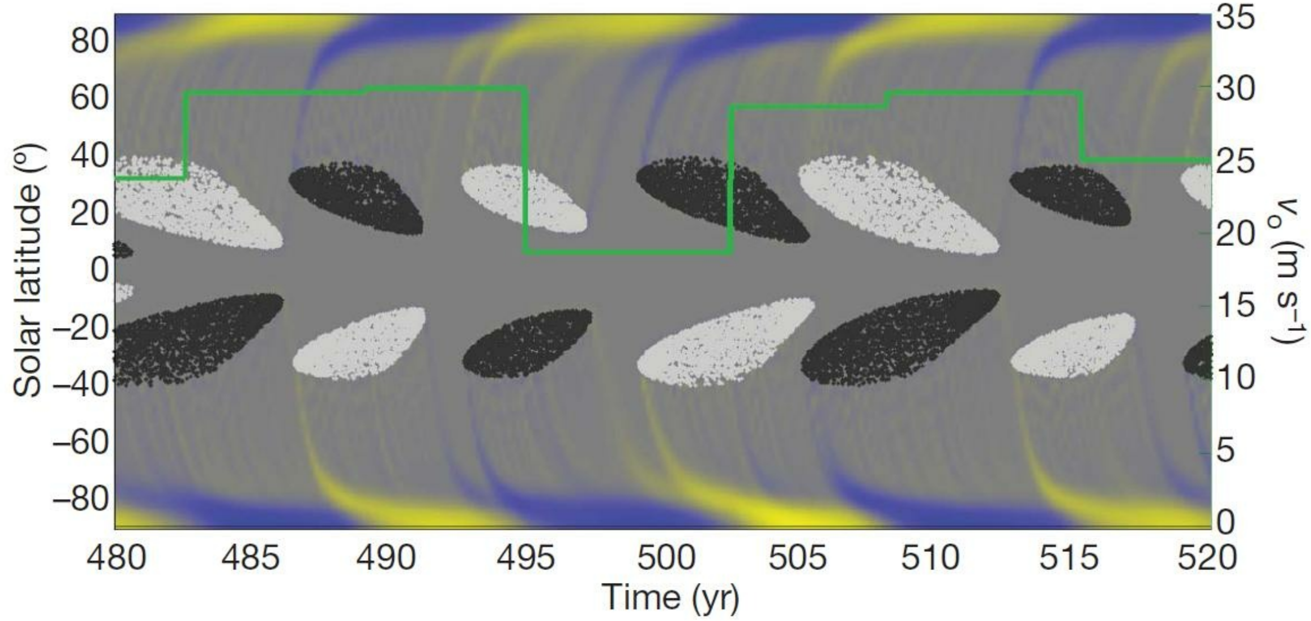

Figure 1 | Simulated sunspot butterfly diagram with a variable meridional flow.

Strike one – the observed meridional flow did the opposite (and they knew it but were told by the editor and referee to not mention it!)

Sunspot Zone Drift

Previous studies had shown a variation in the latitude of the sunspot zones and their equatorward drift rate depending on the size of the cycle. Recently Hathaway *Solar Phys.* 273, 221 (2011) showed that this variability disappeared when time is measured relative to the starting time of each cycle.

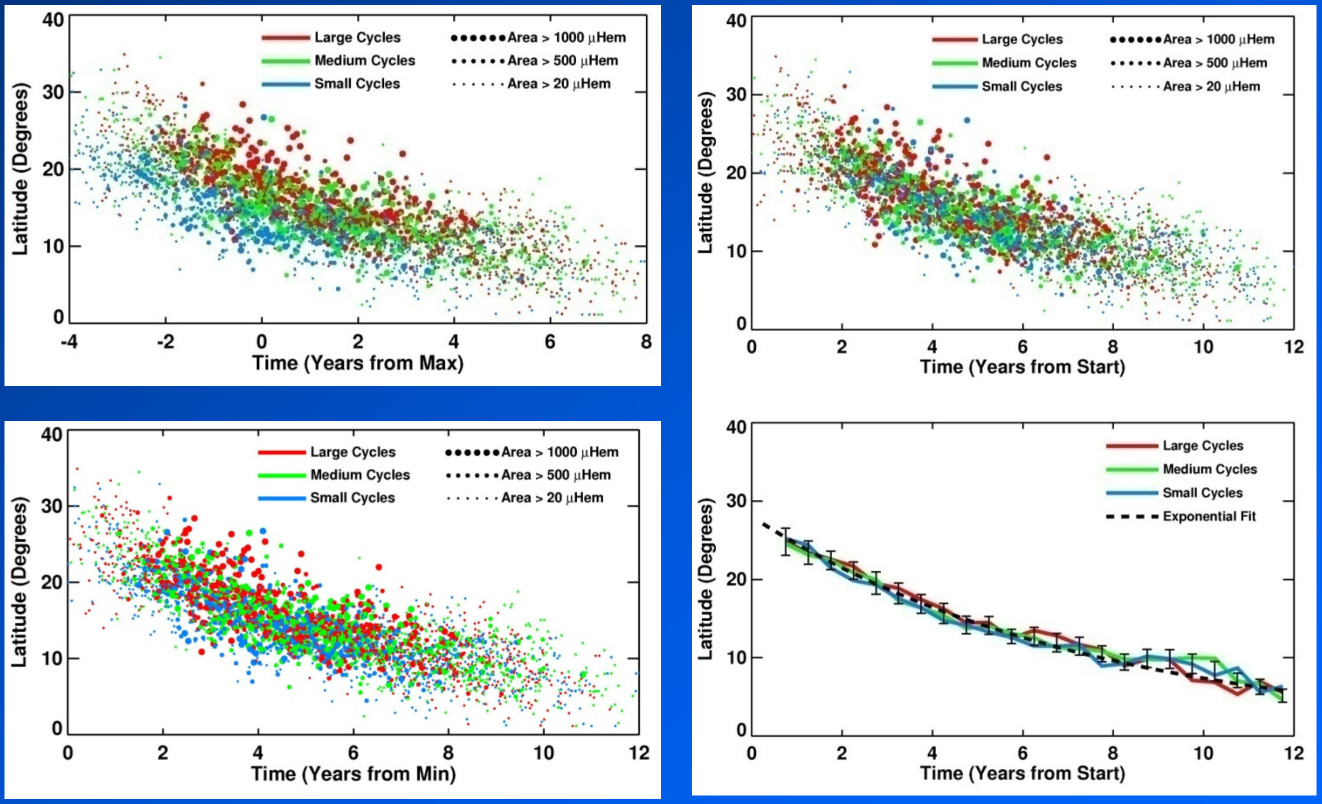

Cycle 23 Behavior

Strike two – the equatorward drift is directly related to the meridional flow speed. No variations are seen from cycle to cycle and both the observed meridional flow speeds and the “desired” meridional flow speeds for cycle 23 are inconsistent with the observations.

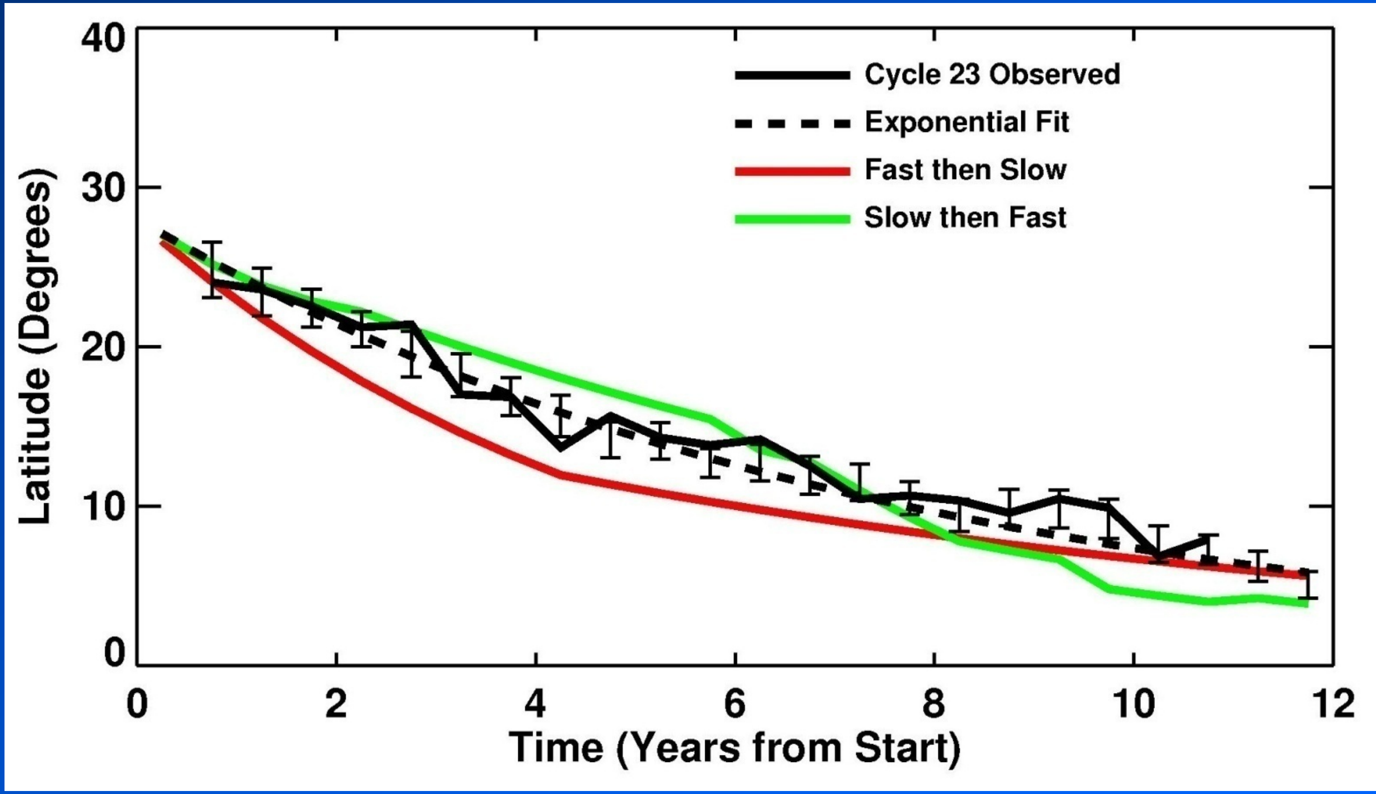

Supergranule Motion Analysis

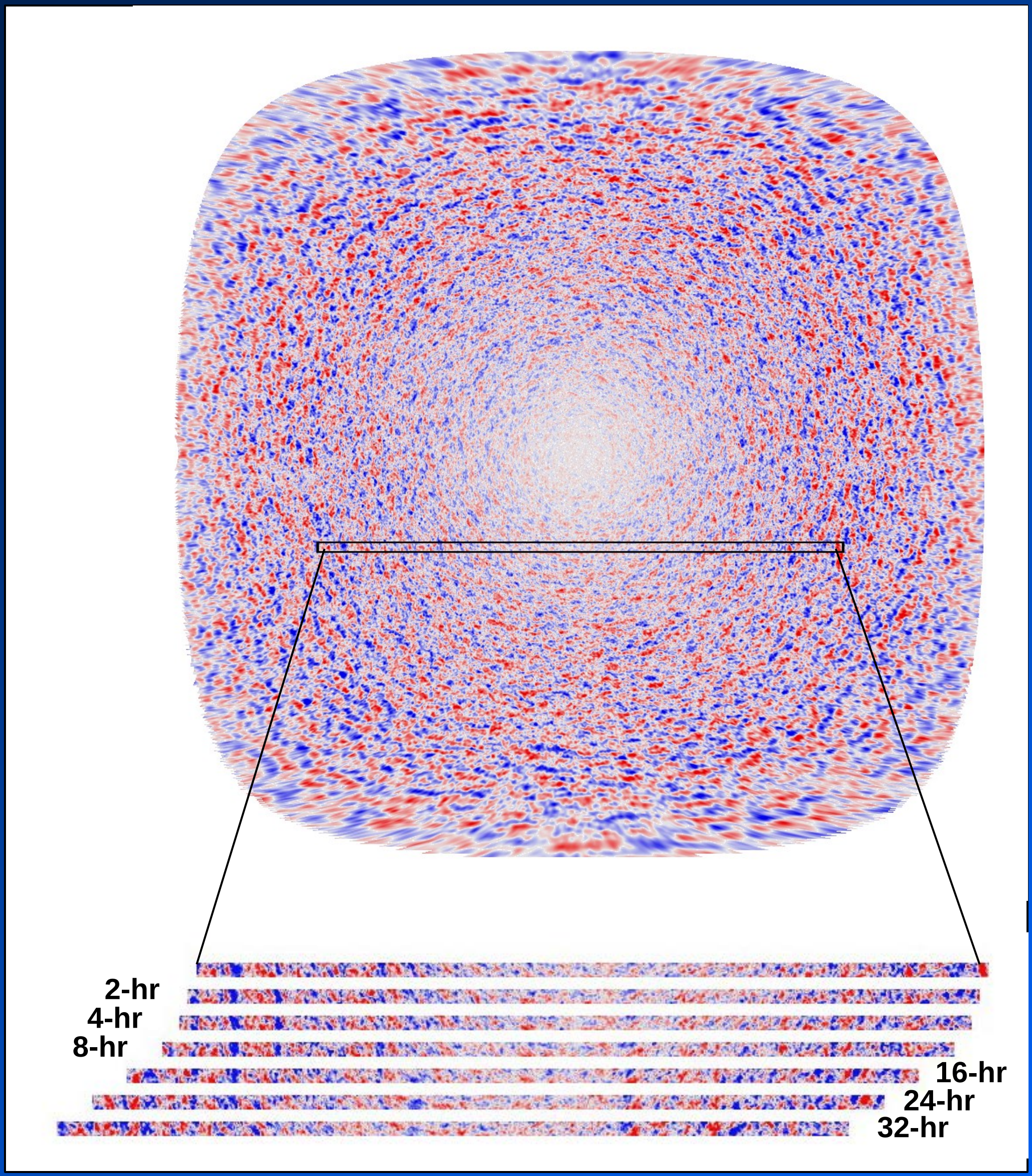

Hathaway et al. (2010) measured the axisymmetric motions of supergranules by cross-correlating 11x600 pixel strips at 860 latitude positions between ±75° from Doppler velocity images acquired at 60-minute intervals by MDI on SOHO and averaging over each of two 60-day observing runs – one in 1996 and another in 1997.

Time is used to filter out smaller and smaller Doppler features by using time lags of 1, 2, 4, 8, 16, 24, and 32 hours.

Depth vs. Wavelength

The Doppler velocity pattern is subject to projection effects (Hathaway et al. *ApJ* 644, 598, 2006). The longitudinal velocities near the equator are multiplied by sin(φ), where φ is the longitude relative to the central meridian. Dividing by this factor and doing a 2D FFT (longitude and time) of equatorial Doppler data gives a rotation velocity as a function of wavelength that matches the rotation velocity as a function of depth. Comparing the rotation velocity from the 2D FFT for raw Doppler data to the rotation velocity found from the cross-correlation analysis gives a correspondence between time-lag and wavelength/depth.

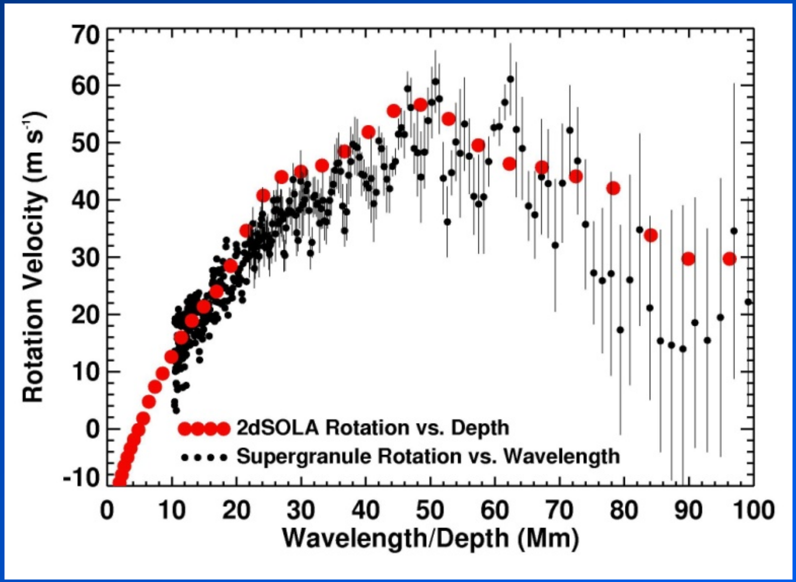

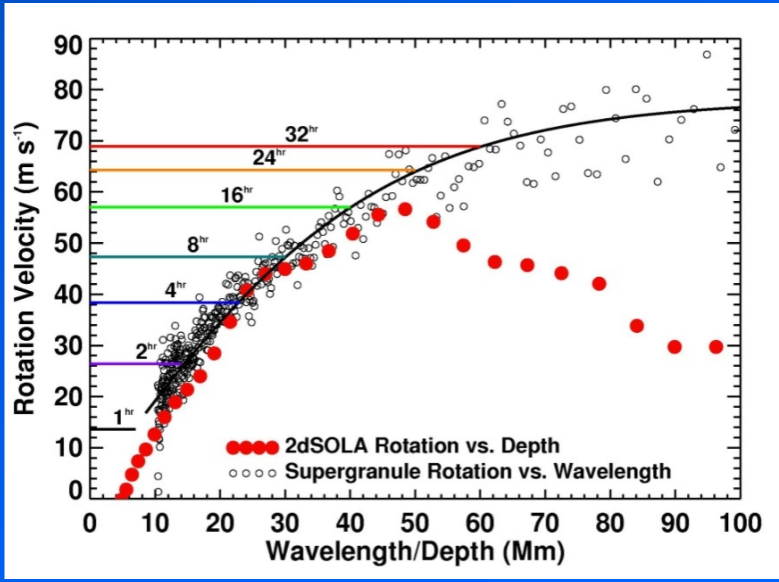

Supergranule Meridional Flow

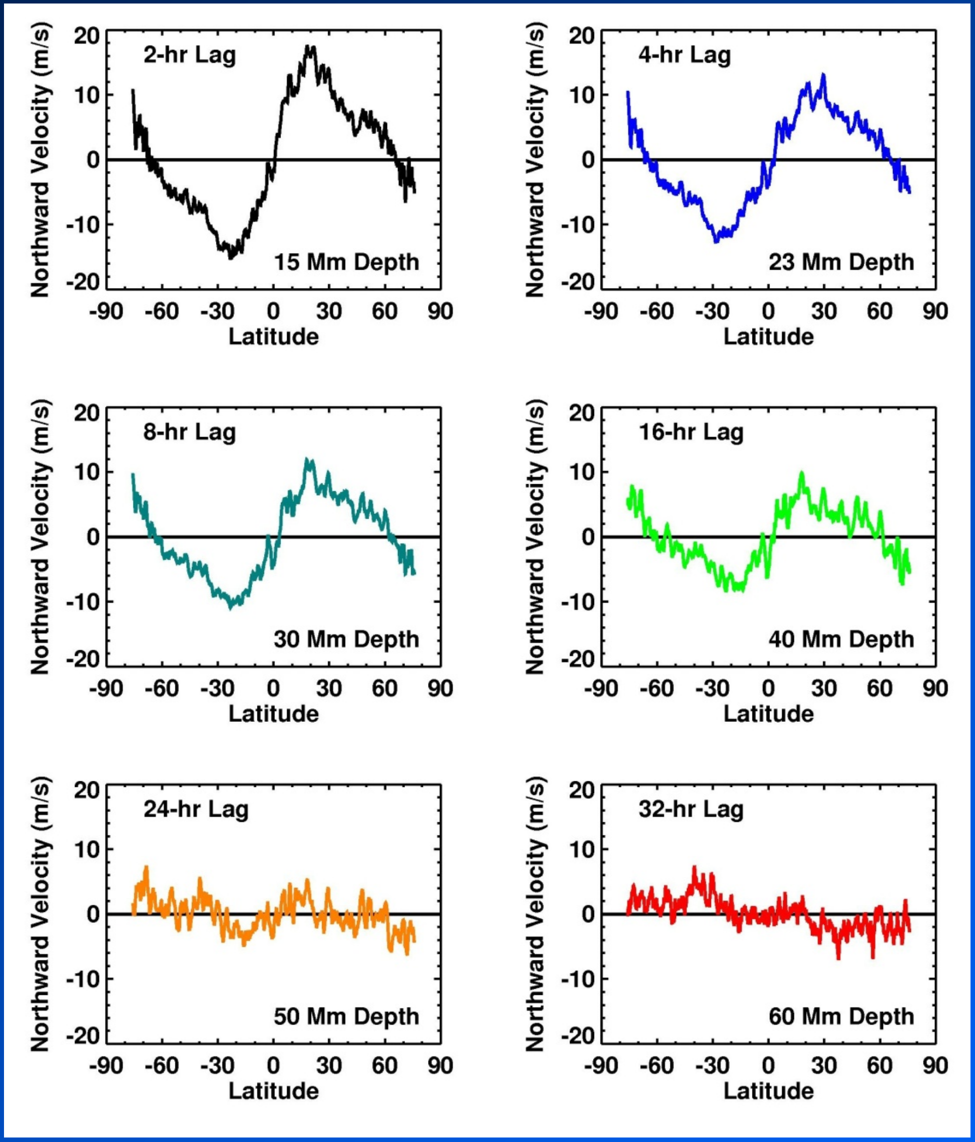

As the time-lag increases from 1-hr to 24-hr, the cells that have those respective lifetimes are transported by a meridional flow that weakens and disappears at 24-hr (50 Mm).

The meridional transport of the cells reverses for the cells with lifetimes of 32-hr (60 Mm).

This is a 10σ detection of the meridional return flow. The poleward meridional flow is confined to the 50 Mm depth of the surface shear layer and returns equatorward just below.

The Shallow Meridional Circulation

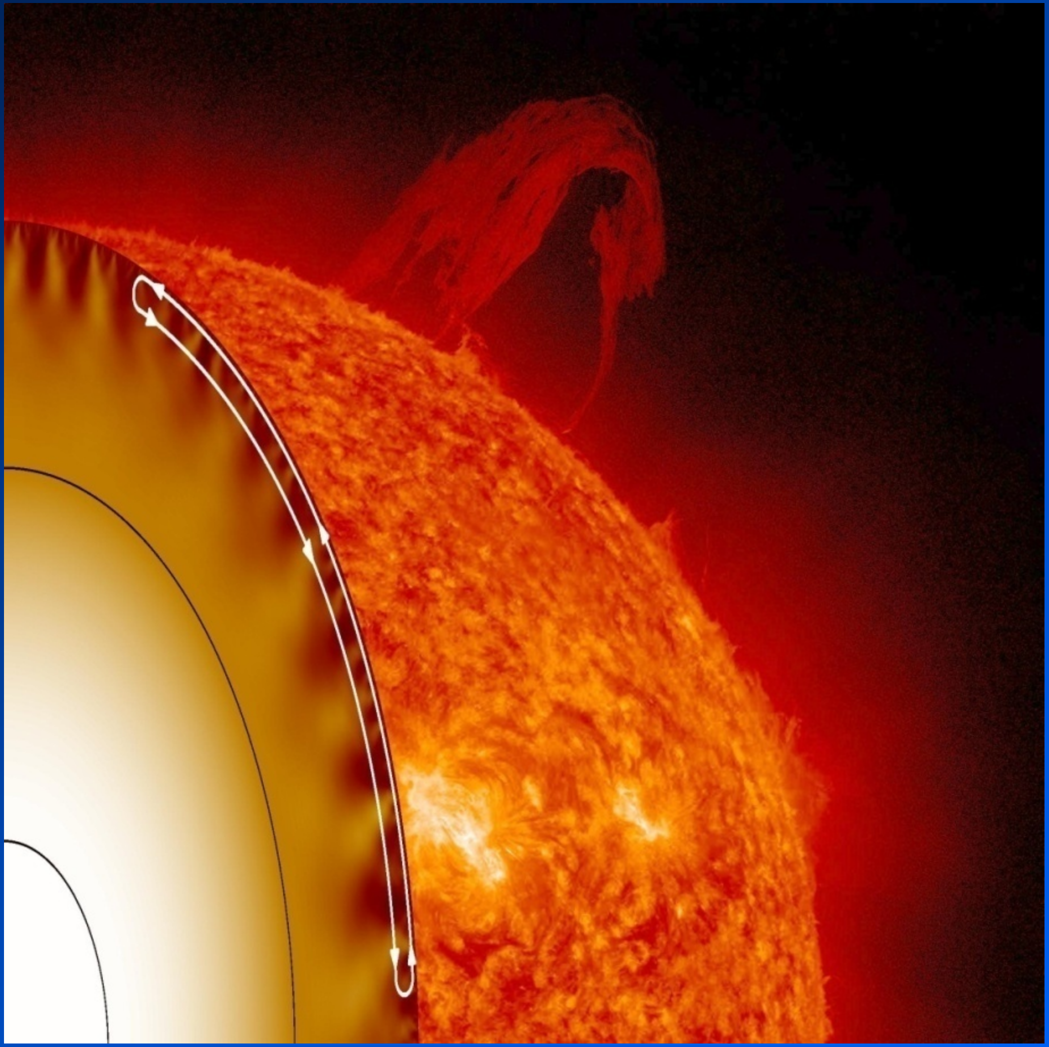

Strike three – the meridional flow does not reverse at a depth of 100 Mm as is assumed in Flux Transport Dynamos.

The equatorward flow at the base of the convection zone must be far less than 1-2 m/s required by Flux Transport Dynamos to give the equatorward drift of the sunspot zones.

Chapter 12:

Directions out of Bankruptcy

What Works?

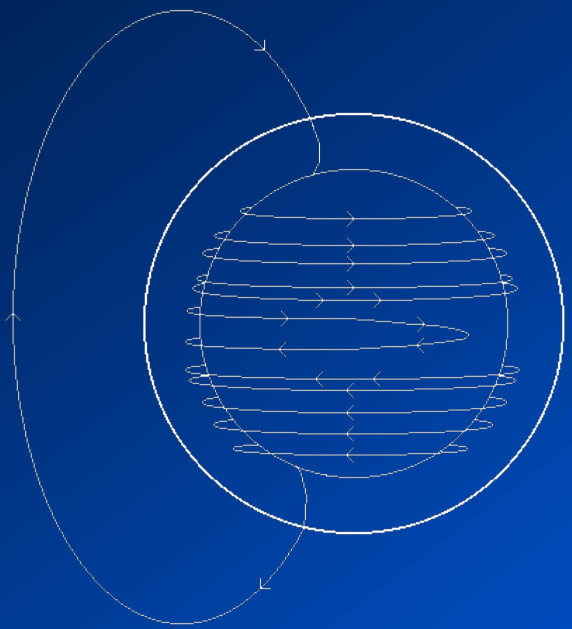

Two processes are common to nearly all solar dynamos-

Differential rotation (rotational shear in either latitude or radius) stretches out (poloidal) field lines in the longitudinal (toroidal) direction – The Omega Effect

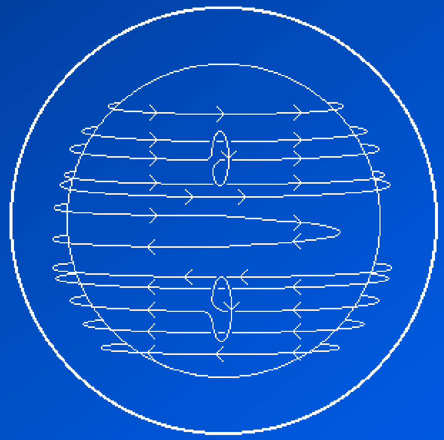

Lifting and twisting of these field lines by non-axisymmetric motions takes the intensified longitudinal (toroidal) fields and rotates them back into meridional (poloidal) direction – The Alpha Effect

Polar Fields Prediction

The strength of the Sun's polar fields near the time of sunspot cycle minimum is expected to be a good predictor based on our understanding of the Sun's magnetic dynamo. This has worked very well for the three observed sunspot cycles.

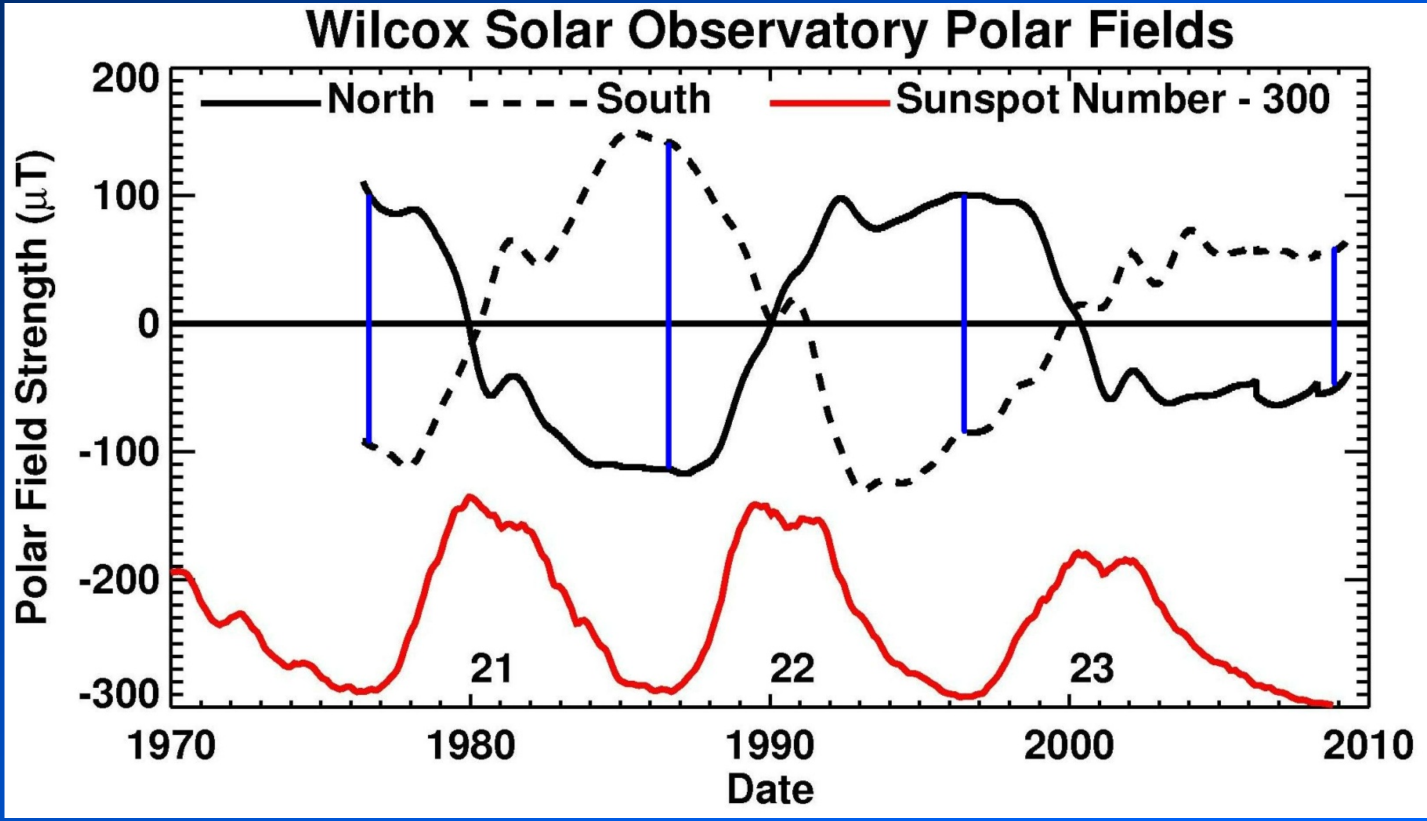

The current very weak polar fields indicate a Cycle 24 peak of 78±20.

Geomagnetic Prediction

The level of the minimum in geomagnetic activity has been one of the best predictors for the size of the next sunspot cycle. First used in 1966, this is thought to be an indicator of polar field strength.

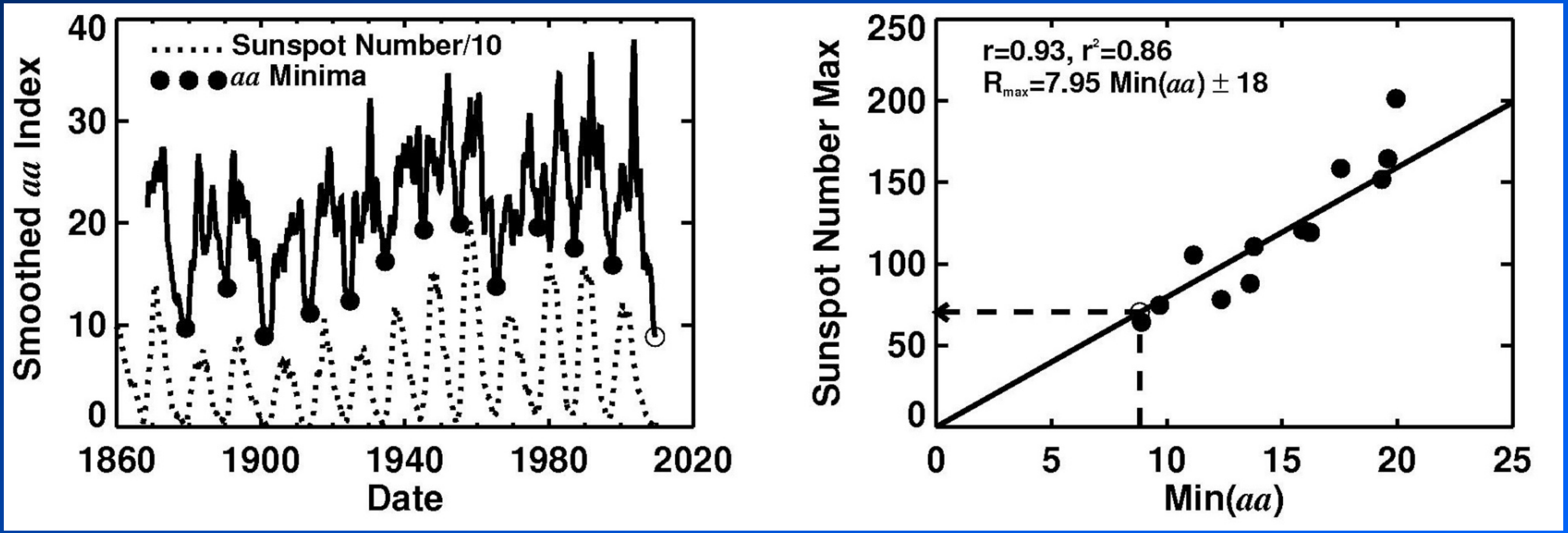

The low geomagnetic activity levels indicate a peak smoothed sunspot number of only 70±18 for Cycle 24.

Surface Flux Transport

Surface magnetic flux transport models were developed in the mid-1980s and showed that, given the emergence of sunspots and their magnetic flux, the subsequent transport of this flux across the surface of the Sun by Differential Rotation, Poleward Meridional Flow, and Supergranule Diffusion could reproduce the observed magnetic field patterns – including the polar magnetic fields.

One problem with these models was that the meridional flow and the supergranule diffusion were poorly constrained so they were free to choose what ever worked. These flows are now well constrained.

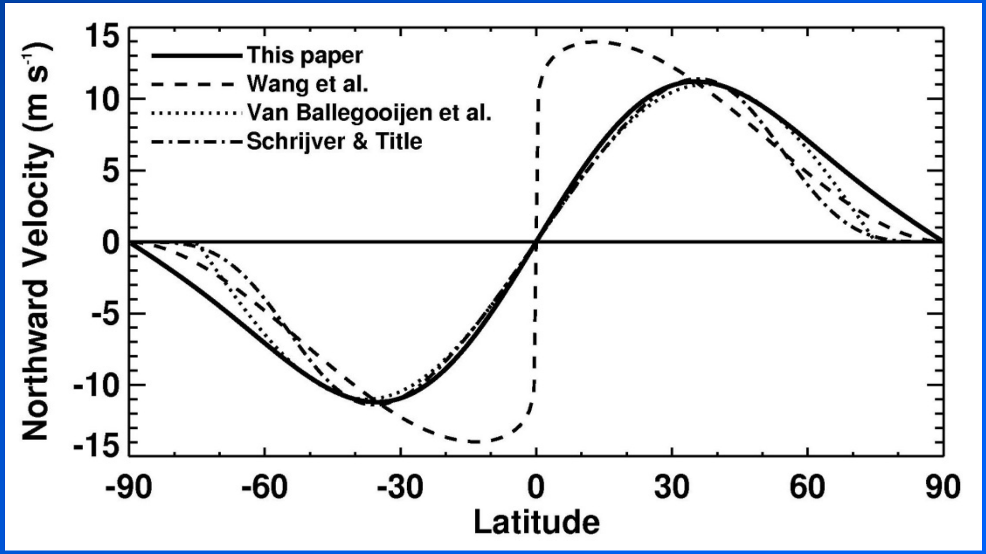

Supergranules

Supergranules cover the entire solar surface. These flows are largely in the horizontal across the surface and are best seen in the Doppler velocity signal they produce. Typical supergranules are about 30,000 km across and last for about 24-hours.

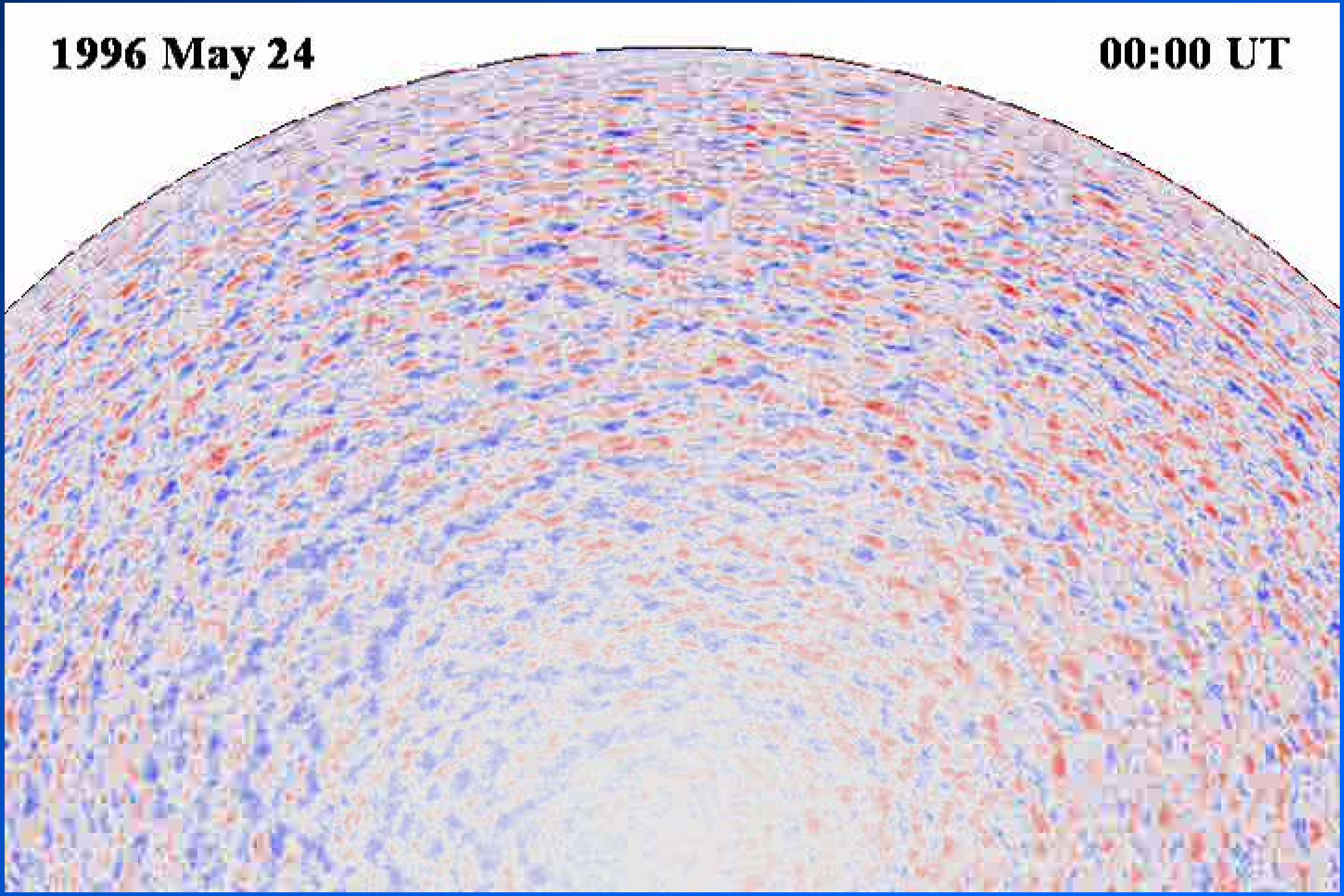

Characterizing Supergranules

Hathaway et al. *ApJ* 725, 1082 (2010) analyzed and simulated Doppler velocity data from MDI to determine the characteristics of supergranulation. These cellular flows have a broad spectrum characterized by a peak in power at wavelengths of about 35 Mm.

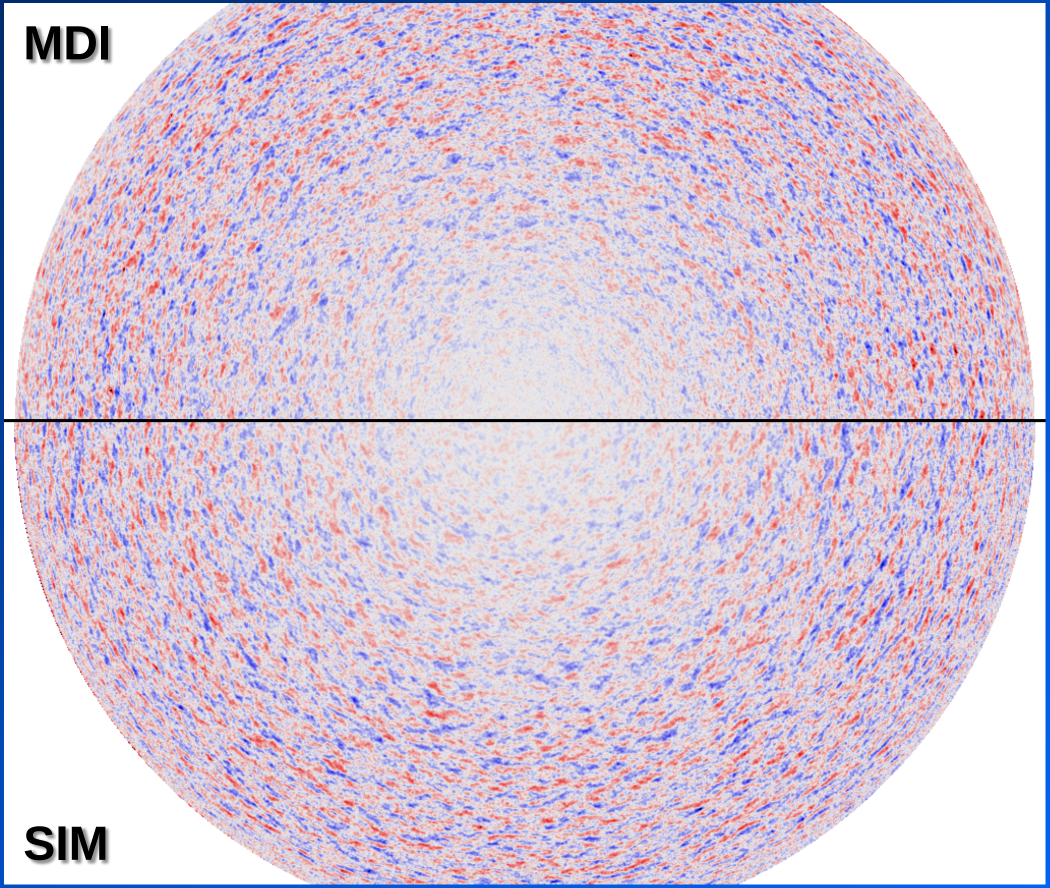

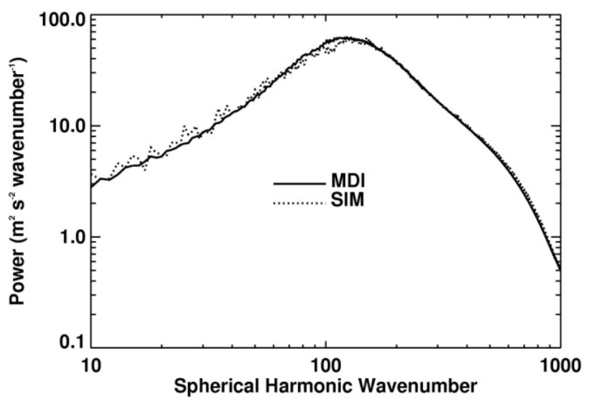

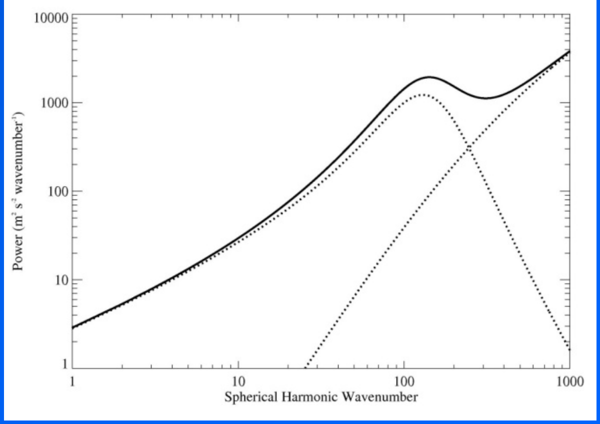

Synchronic Map Construction

Flux is advected by the differential rotation and meridional flow observed for each solar rotation, and by the average of 4 realizations of the supergranule velocity pattern. Full disk data is then assimilated with weights that vary inversely with noise and decay exponentially with time.

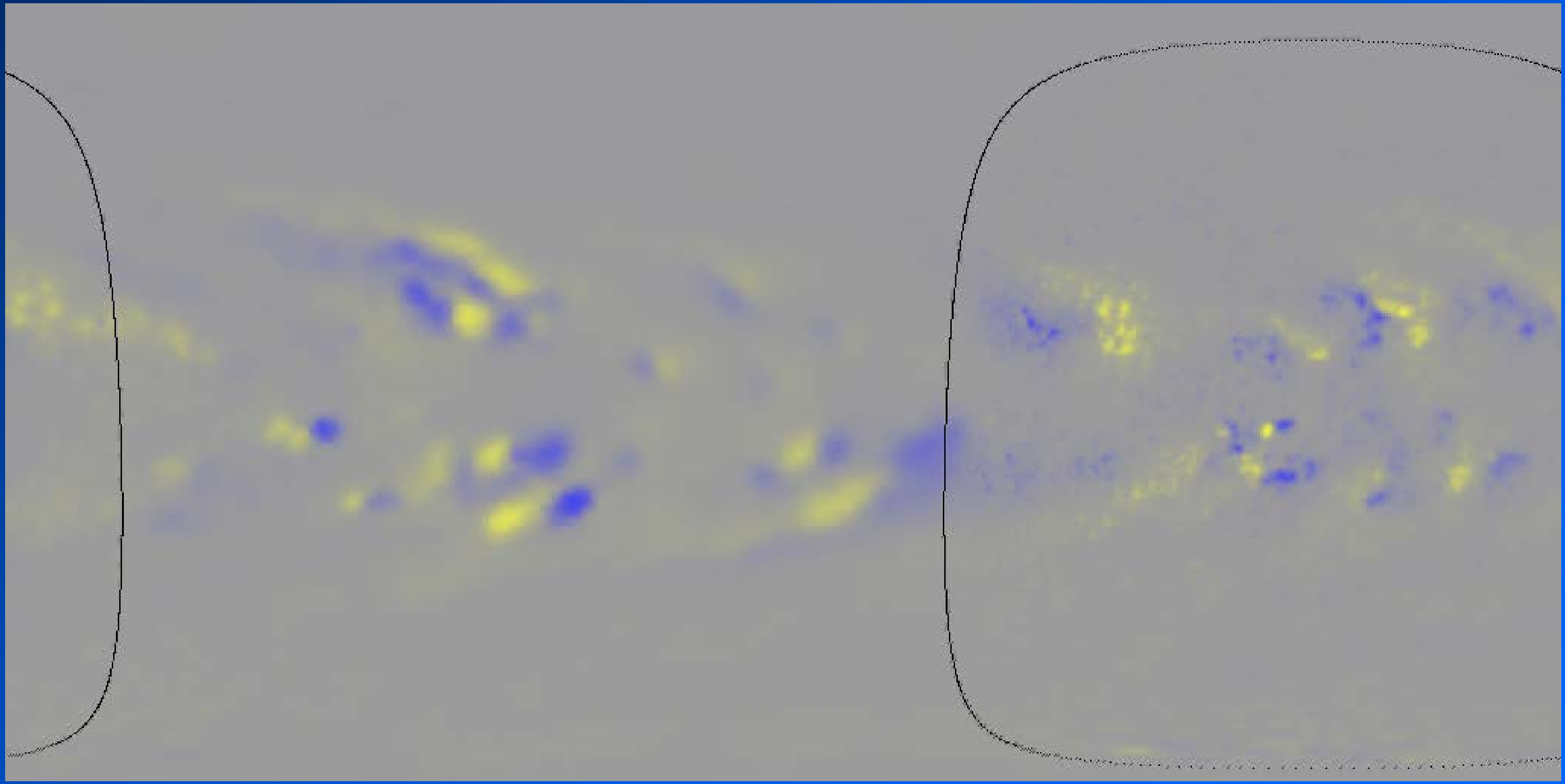

Updated 15 times per day

An SSL (Surface Shear Layer) Dynamo?

The Surface Shear Layer has many features needed for the solar dynamo.

1. A rotation rate that increases inward (needed to give an equatorward dynamo wave)
2. Poleward meridional flow and supergranule diffusion (needed to give the polar field reversals)
3. Variations in the meridional flow (needed to produce variations in the polar fields and variations in cycle strength)
4. A meridional flow that varies with activity (needed for nonlinear feedback)

A problem area is keeping the normally buoyant magnetic flux in the layer and producing the Joy's Law tilt of active regions

1. "Topological Pumping" (concentrated downdrafts/distributed updrafts) could keep magnetic flux within the layer
2. The latitudinal differential rotation could give the Joy's Law tilt as in Babcock (1961)

Conclusions

- Flux Transport Dynamos have three strikes against them:
  1. The observed Cycle 23 meridional flow variations are opposite to what these models required to explain Cycle 23 behavior
  2. The equatorward drift of the sunspot zones follows a standard law which does not vary with cycle strength, length, or meridional flow speed
  3. The meridional circulation is shallow, it turns equatorward at a depth of 50 Mm not 100 Mm

- The surface shear layer itself may play a more significant role in the solar dynamo